THE JOURNAL OF BIOLOGICAL CHEMISTRY VOL. 290, NO. 52, pp. 30813–30829, December 25, 2015

Telomerase Deficiency Causes Alveolar Stem Cell Senescence-associated Low-grade Inflammation in Lungs*

Received for publication, August 1, 2015, and in revised form, October 30, 2015 Published, JBC Papers in Press, October 30, 2015, DOI 10.1074/jbc.M115.681619

Ruping Chen[‡§], Kexiong Zhang[§], Hao Chen[§], Xiaoyin Zhao[§], Jianqiu Wang[§], Li Li[§], Yusheng Cong[§], Zhenyu Ju[§], Dakang Xu[§¶‖], Bryan R. G. Williams[¶‖], Jihui Jia[‡], and Jun-Ping Liu[‡§¶‖1]**

*From the [‡]Department of Microbiology/Key Laboratory for Experimental Teratology of Chinese Ministry of Education, School of Medicine, Shandong University, Jinan, Shandong Province 250012, China, the [§]Institute of Aging Research, Hangzhou Normal University, School of Medicine, Hangzhou, Zhejiang Province 311121, China, the [¶]Hudson Institute of Medical Research, Clayton, Victoria 3168, Australia, the [‖]Department of Molecular and Translational Science, Faculty of Medicine, Monash University, Clayton, Victoria 3168, Australia, and the **Department of Immunology, Faculty of Medicine, Central Clinical School, Monash University, Prahran, Victoria 3018, Australia*

Mutations of human telomerase RNA component (*TERC*) and telomerase reverse transcriptase (*TERT*) are associated with a subset of lung aging diseases, but the mechanisms by which TERC and TERT participate in lung diseases remain unclear. In this report, we show that knock-out (KO) of the mouse gene *Terc* or *Tert* causes pulmonary alveolar stem cell replicative senescence, epithelial impairment, formation of alveolar sacs, and characteristic inflammatory phenotype. Deficiency in TERC or TERT causes a remarkable elevation in various proinflammatory cytokines, including IL-1, IL-6, CXCL15 (human IL-8 homolog), IL-10, TNF-α, and monocyte chemotactic protein 1 (chemokine ligand 2 (CCL2)); decrease in TGF-β1 and TGFβRI receptor in the lungs; and spillover of IL-6 and CXCL15 into the bronchoalveolar lavage fluids. In addition to increased gene expressions of α-smooth muscle actin and collagen 1α1, suggesting myofibroblast differentiation, TERC deficiency also leads to marked cellular infiltrations of a mononuclear cell population positive for the leukocyte common antigen CD45, low-affinity Fc receptor CD16/CD32, and pattern recognition receptor CD11b in the lungs. Our data demonstrate for the first time that telomerase deficiency triggers alveolar stem cell replicative senescence-associated low-grade inflammation, thereby driving pulmonary premature aging, alveolar sac formation, and fibrotic lesion.

Telomerase is a ribonucleoprotein complex that operates to maintain telomeres (chromosomal ends), counteracting cell division-associated telomere shortening in the stem cell compartment and cancer (1, 2). Loss-of-function gene mutations on telomerase subunits occur in a number of diseases (3, 4), including dyskeratosis congenita (5, 6), aplastic anemia (7, 8), liver cirrhosis (9, 10), and idiopathic pulmonary fibrosis (IPF)[2] (11–14). This association of telomerase gene mutations with aging-related diseases of various tissues may implicate telomerase as playing a key role in undifferentiated stem cells of different tissues to prevent the specific tissues from premature aging. Thus, telomerase loss of function is considered to be a key risk factor in causing telomere dysfunction and premature replicative senescence of tissue stem cells across different tissues and organs (3). A syndrome complex has been demonstrated in a subset of IPF patients with telomerase mutations and increased incidence of bone marrow failure (11). A comorbidity of aplastic anemia, myelodysplasia, leukemia, and pulmonary fibrosis has also been shown to involve telomerase mutations (15), but the mechanisms common to tissue-specific development of pathologies following telomerase mutations remain unclear (16, 17).

Experimental studies on animals have demonstrated certain causal roles of telomerase deficiency in compromised tissue homeostasis and dysfunctional organs (18–21). Knock-out of telomerase RNA component (TERC) or telomerase reverse transcriptase (TERT) causes the phenotypes resembling dyskeratosis congenita (22, 23) and bone marrow failure (19, 23, 24). In the lungs of TERC-deficient mice, elevated apoptosis of alveolar stem cells (alveolar epithelial type II cells (AECII)) (25), hindered tissue growth in partial pneumonectomies (26). Furthermore, an increased susceptibility to cigarette smoke-associated emphysematous changes that is independent of cigarette smoking-induced increases in alveolar macrophages (27) has been shown. Intriguingly, mice with TERC deficiency and short telomeres do not show obvious pulmonary fibrosis (27), whereas mice that have developed pulmonary fibrosis from bleomycin insult require telomerase activity (28–30), mirroring the findings that the majority of IPF lung samples showed increased telomerase activity (30).

* This work was supported by National Basic Research Program of China Grant 2012CB911204, National Natural Science Foundation of China Grants 81170313 and 81272889, National Health and Medical Research Council of Australia Grant 1051882, and the Victorian Government's Operational Infrastructure Support Program. The authors declare that they have no conflicts of interest with the contents of this article.

[1] To whom correspondence should be addressed. E-mail: jun-ping.liu@monash.edu.

[2] The abbreviations used are: IPF, idiopathic pulmonary fibrosis; TERC, telomerase RNA component; TERT, telomerase reverse transcriptase; APC, allophycocyanin; PE, phycoerythrin; AECI and AECII, alveolar epithelial type I and II cell(s), respectively; α-SMA, α-smooth muscle actin; Col1α1, collagen type 1 α1; BAL, bronchoalveolar lavage; CCL2, chemokine ligand 2; TIF, telomere dysfunction-induced focus; SPC, surfactant protein-C; EpCAM, epithelial cell adhesion molecule; DDR, DNA damage response; HP1γ, heterochromatin protein 1γ; SALI, senescence-associated, low-grade inflammation; SASP, senescence-associated secretory phenotype; tSASP, telomere-induced SASP; tSALI, telomere-induced SALI; NK, natural killer; G1, G2, and G3, generation 1, 2, and 3, respectively.

To investigate how telomerase participates in the development of pulmonary aging-associated disorders, we reasoned that telomerase deficiency initiates alveolar stem cell telomere loss-induced replicative senescence and a proinflammatory microenvironment to drive further abnormalities. Using TERC or TERT knock-out (KO) mice, we found a significant increase in the aging populations of AECII with a marked reduction in the total AECII number in the lungs. Increased gene expressions of α-smooth muscle actin (α-SMA) and collagen type 1 α1 (Col1α1) occurred to the telomerase-deficient pulmonary interstitium, and several inflammatory cytokines were markedly increased in the bronchoalveolar lavage (BAL) fluids of TERC KO mice, including IL-6, CXCL15, tumor necrosis factor-α (TNF-α), and monocyte chemotactic protein-1 (also known as chemokine ligand 2 (CCL2)). Furthermore, a number of cell populations positive for the leukocyte common antigen CD45, low-affinity Fc receptor CD16/CD32, or pattern recognition receptor CD11b were remarkably detected at significant levels in the lungs of TERC KO mice. The data demonstrate for the first time a telomerase deficiency- and telomere shortening-induced pattern of pulmonary alveolar stem cell replicative senescence-associated low-grade inflammation in lung tissues. The innate immune response, including extracellular accumulations of proinflammatory cytokines, mononuclear immune cells, and differentiated myofibroblasts, may underlie the development of pulmonary premature aging and aging-related disorders.

Experimental Procedures

Animals and AECII Isolation—All of the mice used were on the C57BL/6J genetic background. Wild type mice, homozygous TERT-null mice (31), and homozygous TERC-null mice (18) were kept in the Animal Experimental Center of Hangzhou Normal University. Mating of generation 1 ($G1^{-/-}$) mice to each other generated generation 2 ($G2^{-/-}$), and $G2^{-/-}$ mice mated to produce $G3^{-/-}$ mice. Wild type *Tert* or wild type TERC mice were used as control. G2 or G3 TERC-null mice at 2.5–3 months old and G3 TERT-null mice at 9 months old were tested with comparable ages of WT mice. Animals were housed in specific pathogen-free (SPF) conditions, bred and maintained at the AEC, Hangzhou Normal University. All animal experiments were approved by the Animal Care and Ethics Committee at Hangzhou Normal University.

Isolation of murine AECII was done by following the published protocol (32, 33). First, Mice were anesthetized with 1% of sodium pentobarbital through intraperitoneal injection (70 μl/10 g). Then the abdominal aorta was intersected, and mice were perfused through the right ventricle with 10 ml of PBS to reduce lung blood content. Dispase (1 ml, 0.25% in DMEM) was injected into the lung to initiate tissue digestions. The lungs were removed from the chest, separated from the heart and thymus, cleaned from connective tissue, and immerged in 1 ml of 0.25% dispase for incubation at 37 °C for 2 h. The pulmonary lobes were dissected into small pieces and filtered with a nylon membrane. The pulmonary cells were stained with APC-labeled epithelial cell adhesion molecule (EpCAM) (Biolegend), PE-CY5.5-CD45 (Biosciences), and PE-T1α (podoplanin) (Biolegend) antibodies, followed by elimination of red blood cells using a lysis buffer (BD Biosciences). Cells were sorted by a flow cytometer (Influx, BD Biosciences). AECII were captured as EpCAM-positive and CD45- and podoplanin-negative cells for further analysis.

Telomere Fluorescence in Situ Hybridization (FISH)—The sorted AECII were attached to microscope glass slides using a cytospin machine (Thermo); fixed at −20 °C in 100% cold methanol for 10 min; dehydrated in ethanol with 70, 95, and 100% EtOH for 5 min consecutively; and air-dried for ~2 min. A hybridizing solution (70% formamide, 0.5% blocking reagent, 10 mM Tris-HCl, pH 7.2) containing the Cy3-labeled peptide nucleic acid probe (Panagene, F1002) was added to each slide. The cells were denatured by heating for 10 min at 80 °C on a heat block and were incubated in the dark overnight at 4 °C. Cells were washed twice with 70% (v/v) formamide, 10 mM Tris-HCl, pH 7.2, before three washes in PBS. The cells were air-dried for a few minutes before DNA was counterstained with DAPI. The telomere signals from Cy3-peptide nucleic acid were captured with an AxioImager M2 microscope (Carl Zeiss), a ×63 oil objective, and Metafer 4 software (Metasystems, Germany).

Telomere Dysfunction-induced Focus (TIF) Analysis—Cells were incubated with primary antibody for 1 h at room temperature and washed in PBS three times for 10 min each, followed by secondary antibody incubation in blocking solution for 30 min at room temperature. Cells were fixed with 2% (w/v) paraformaldehyde for 5 min at room temperature; washed in PBS twice; dehydrated in ethanol with 70, 95, and 100% EtOH for 5 min consecutively; and dried in air. The rest procedure was same as in the FISH protocol. For statistical analysis, more than two 53BP1 signals co-localized with telomere signals were captured with a deconvolution microscope (DeltaVision, Applied Precision).

Senescence Analysis by β-Galactosidase (β-Gal) Staining—β-Galactosidase staining was performed to detect senescent cells by incubating cells with 200 μl of staining mixture per tissue stock on slides (1 mg/ml X-gal solution, 5 mM potassium ferrocyanide, 5 mM potassium ferricyanide, 20 μl of 10× staining solution, pH 6.0). The stained slides were incubated in a sealed and wet box at 37 °C for 24 h. Slides were soaked in hot PBS on a shaker to dissolve the precipitated crystal for a clean background and counterstained with nuclear fast red solution for 30 min at room temperature. The cells were rinsed and sealed by resin for observation under the microscope.

Flow Cytometric β-Galactosidase Activity Analysis—To measure β-galactosidase activity in AECII by flow cytometry, pulmonary lobes were digested by dispase. Pulmonary cell suspension was incubated with chloroquine at 37 °C for 1 h and then with fluorogenic substrate C12FDG for 20 min at 37 °C. Membrane-permeable C12FDG is a non-fluorescent substrate of β-galactosidase and emits green fluorescence after hydrolysis of the galactosyl residues and becomes confined within the cell (34). The incubation was stopped with prechilled PBS, which was followed by incubating the cell suspension with AECII markers at 4 °C for 40 min. Cells were loaded on a Fotessa flow cytometer (BD Biosciences). Data were acquired and analyzed with Flowjo software.

TABLE 1
Primer sequences used in quantitative PCR analysis

Gene name	Oligonucleotide name	Primer sequence
Spc	q-m-Sftpc-f	Forward: 5′-CCTCGTTGTCGTGGTGAT-3′
	q-m-Sftpc-r	Reverse: 5′-GGTAGCGATGGTGTCTGC-3′
Podoplanin (T1α)	q-m-T1α-f	Forward: 5′-TCCACCTCAGCAACCTC-3′
	q-m-T1α-r	Reverse: 5′-GCTAACAAGACGCCAACTA-3′
P15	q-m-p15-f	Forward: 5′-AGATCCCAACGCCCTGAAC-3′
	q-m-p15-r	Reverse: 5′-CCCATCATCATGACCTGGATT-3′
P16	q-m-p16-f	Forward: 5′-CATCTGGAGCAGCATGGAGTC-3′
	q-m-p16-r	Reverse: 5′-GGGTACGACCGAAAGAGTTCG-3′
P21	q-m-p21-f	Forward: 5′-CCAATCCTGGTGATGTCCG-3′
	q-m-p21-r	Reverse: 5′-TCAAAGTTCCACCGTTCTCG-3′
Acta2 (α-SMA)	q-m-αSMA-f	Forward: 5′-CCGAGCGTGAGATTGTCC-3′
	q-m-αSMA-r	Reverse: 5′-CGTCAGGCCAGTTCGTAGC-3′
Col1a1	q-m-Col1a1-f	Forward: 5′-CCTACTCAGCCGTCTGTGCC-3′
	q-m-Col1a1-r	Reverse: 5′-AGCCCTCGCTTCCGTACTCG-3′
Tgfβ1	q-m-Tgfb1-f	Forward: 5′-GAAGCAGTGCCCGAACC-3′
	q-m-Tgfb1-f	Reverse: 5′-AGCCACTCAGGCGTATCAG-3′
Tgfβri	q-m-Tgfbr1-f	Forward: 5′-CAGCTCCTCATCGTGTTGGT-3′
	q-m-Tgfbr1-r	Reverse: 5′-CAGAGGTGGCAGAAACACTG-3′
Tgfβrii	q-m-Tgfbr2-f	Forward: 5′-ATGCATCCATCCACCTAAGC-3′
	q-m-Tgfbr2-r	Reverse: 5′-TGTCGCAAGTGGACAGTCTC-3′
Bmpria	q-m-Bmpr1a-f	Forward: 5′-CTTCTCCAGCTGCTTTTGCT-3′
	q-m-Bmpr1a-r	Reverse: 5′-AACGACCCCTGCTTGAGATA-3′
Bmprib	q-m-Bmpr1b-f	Forward: 5′-TGTAAATGCCACCACCACTG-3′
	q-m-Bmpr1b-f	Reverse: 5′-TGACAACAGGCATTCCAGAG-3′
Bmprii	q-m-Bmpr2-f	Forward: 5′-ACCGCTTTTGCTGCTGTAGT-3′
	q-m-Bmpr2-r	Reverse: 5′-CAGAAACTGATGCCAAAGCA-3′
Il1α	q-m-IL1a-f	Forward: 5′-TCTGCCATTGACCATCTC-3′
	q-m-IL1a-r	Reverse: 5′-ATCTTCCCGTTGCTTGAC-3′
Il1β	q-m-IL1b-f	Forward: 5′-GCTGAAAGCTCTCCACCTCA-3′
	q-m-IL1b-r	Reverse: 5′-AGGCCACAGGTATTTTGTCG-3′
Il2	q-m-IL2-f	Forward: 5′-AAGCTCTACAGCGGAAGCAC-3′
	q-m-IL2-r	Reverse: 5′-ATCCTGGGGAGTTTCAGGTT-3′
Il6	q-m-IL6-f	Forward: 5′-GTTCTCTGGGAAATCGTGGA-3′
	q-m-IL6-r	Reverse: 5′-TTCTGCAAGTGCATCATCGT-3′
Il8	q-m-IL8-f	Forward: 5′-ATCTTCGTCCGTCCCTG-3′
	q-m-IL8-r	Reverse: 5′-CAACAGTAGCCTTCACCC-3′
Il10	q-m-IL10-f	Forward: 5′-CAGCCGGGAAGACAATAACT-3′
	q-m-IL10-r	Reverse: 5′-ATGTTGTCCAGCTGGTCCTT-3′
Tnfα	q-m-Tnfa-f	Forward: 5′-CCCCAAAGGGATGAGAAGTT-3′
	q-m-Tnfa-r	Reverse: 5′-CACTTGGTGGTTTGCTACGA-3′
Ccl2	q-m-CCL2-f	Forward: 5′-CCCTGTCATGCTTCTGG-3′
	q-m-CCL2-r	Reverse: 5′-TCATTGGGATCATCTTGC-3′
β-Actin	q-m-β-actin-f	Forward: 5′-CAGCCTTCCTTCTTGGGTAT-3′
	q-m-β-actin-r	Reverse: 5′-TGGCATAGAGGTCTTTACGG-3′

Immunofluorescence and Immunohistochemistry Assay—Paraffin slides were dewaxed first and dehydrated before antigen retrieval. Immunofluorescence was processed by fixing, blocking, primary antibody, and then secondary antibody incubation, with final sealing. For immunohistochemistry, avidin was added to the blocking solution, and biotin was added to the primary antibody solution, followed by ABC regents and diaminobenzidine color development and dehydration.

Analysis of mRNA Expression—The total RNA was extracted from mouse pulmonary tissues or other tissues as indicated by the TRIzol classical RNA extraction method. Reverse transcription-PCR was carried out with the primescript^{TM} RT reagent kit (TAKARA, catalog no. RR047A). Quantitative PCR was carried out on an Applied Biosystems 7500 system, using actin as the reference gene. Primers for quantitative PCR are listed in Table 1.

Flow Cytometry and Cell Sorting—Antibodies used for flow cytometry analysis or cell sorting were purchased from eBioscience, Biolegend, or BD Biosciences. The antibody clones and fluorescent labels for FACS analysis are listed in Table 2. After dispase digestion, pulmonary lobes were dissected into smaller pieces and filtered with a nylon membrane. Red blood cells were eliminated by lysing buffer (BD Biosciences), and cells were stained with different combinations of antibodies. Finally, cells were analyzed on a flow cytometer (LSRFortessa, BD Biosciences).

TABLE 2
Antibodies used in FACS

Fluorescence	Antibody	Clone	Company	Catalogue no.
FITC	F4/80	BM8	eBioscience	11-4801-82
FITC	CD4	RM4–5	eBioscience	11-0042-81A
PE	NK1.1	PK136	BD Biosciences	553165
Percp-Cy5.5	CD16/32	93	eBioscience	45-0161-82
Percp-Cy5.5	CD45	30-F11	eBioscience	45-0451-82
APC	Epcam	G8.8	BioLegend	118214
APC	CD11b	M1/70	eBioscience	11-0112-82
APC	CD11c	N418	BioLegend	117309
APC	CD8a	53–6.7	BD Biosciences	553035

BAL Fluid Analysis—The lungs were subjected to perfusion with 1 ml of PBS via a tracheal polyethylene catheter. The BAL fraction was centrifuged at 1,400 $\times$ *g* for 5 min, and the supernatant was harvested to measure cytokine expression by ELISA (35, 36).

Western Blotting—Homogenized lung tissues or isolated AECII were lysed on ice in radioimmune precipitation buffer. Protein concentration was determined using the BCA method. Equal amounts (60 μg) of cell extracts were separated on SDS-

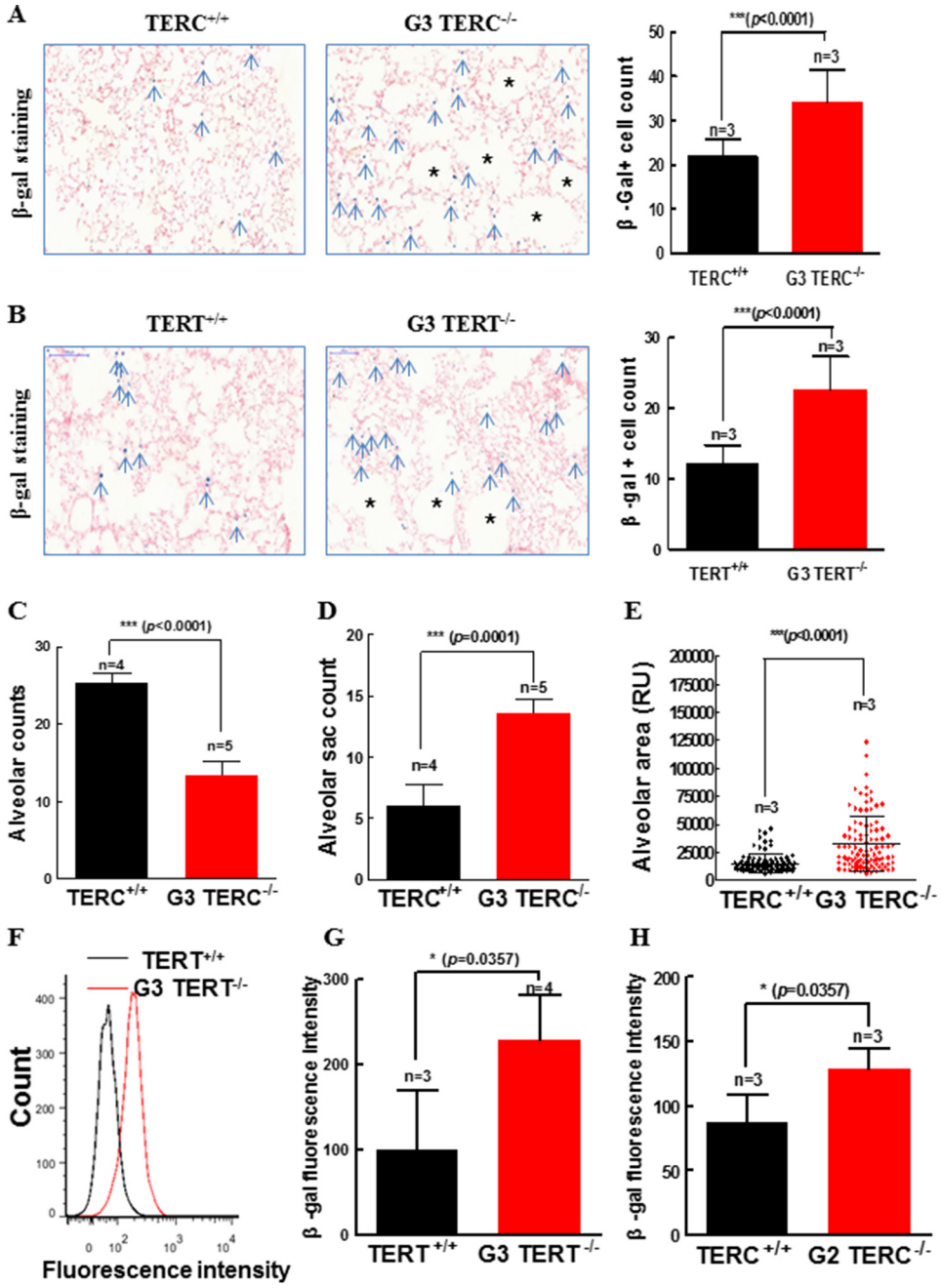

FIGURE 1. **Pulmonary aging induced by TERC or TERT deficiency.** *A*, β-gal staining of pulmonary sections from TERC-null mice. The *left* and *middle panels* are representative micrographs of β-gal staining observed with a ×20 and ×40 objective lens. *Blue arrows*, positive stained cells; *asterisks*, alveolar sacs. The *right bar graph* shows the quantitative data of the β-gal staining from three animals. Data are the mean ± S.E. (*error bars*). *B*, β-gal staining of the pulmonary sections from TERT-null mice. The *left* and *middle panels* are representative micrographs of β-gal staining observed with a ×20 objective lens. *Blue arrows*, positive stained cells; *asterisks*, alveolar sacs. The *right bar graph* shows the quantitative data of the β-gal staining from three animals. Data are the mean ± S.E. *C–E*, comparisons of alveolar counts (*C*), alveolar sac counts (*D*), and total alveolar areas (*E*) between WT and G3 TERC-null lungs. Data are mean ± S.E. from three experiments. *F–H*, SA-β-gal activity in AECII was detected by flow cytometry with incubation of C12FDG and AECII markers. *RU*, relative units.

PAGE and transferred to PVDF membranes (Millipore) for antibody blotting. The following antibodies were used: α-SMA (Sigma, A2547), surfactant protein-C (SPC) (Abcam, 90716), and p53 (Abcam, ab26). 10,000–30,000 isolated AECII were lysed with 35 μl of radioimmune precipitation assay buffer and used in each assay.

Statistical Analysis—Two-tailed or one-tailed unpaired Student's *t* tests were applied for comparisons between the means of various groups. A *p* value of <0.05 was considered statistically significant.

Results

Deficiency of Terc or Tert Gene Resulted in AECII Replicative Senescence and Pulmonary Aging—Mice carrying a deletion of the *mTerc* or *mTert* gene on a C57BL/6J background were examined at the ages of 2.5–3 months for tissue and cellular markers of aging. In the lung sections stained for β-gal in TERC-null and TERT-null mice (Fig. 1, *A* and *B*), microscopic examination revealed significant changes in morphological structures in the pulmonary alveoli. These changes involved

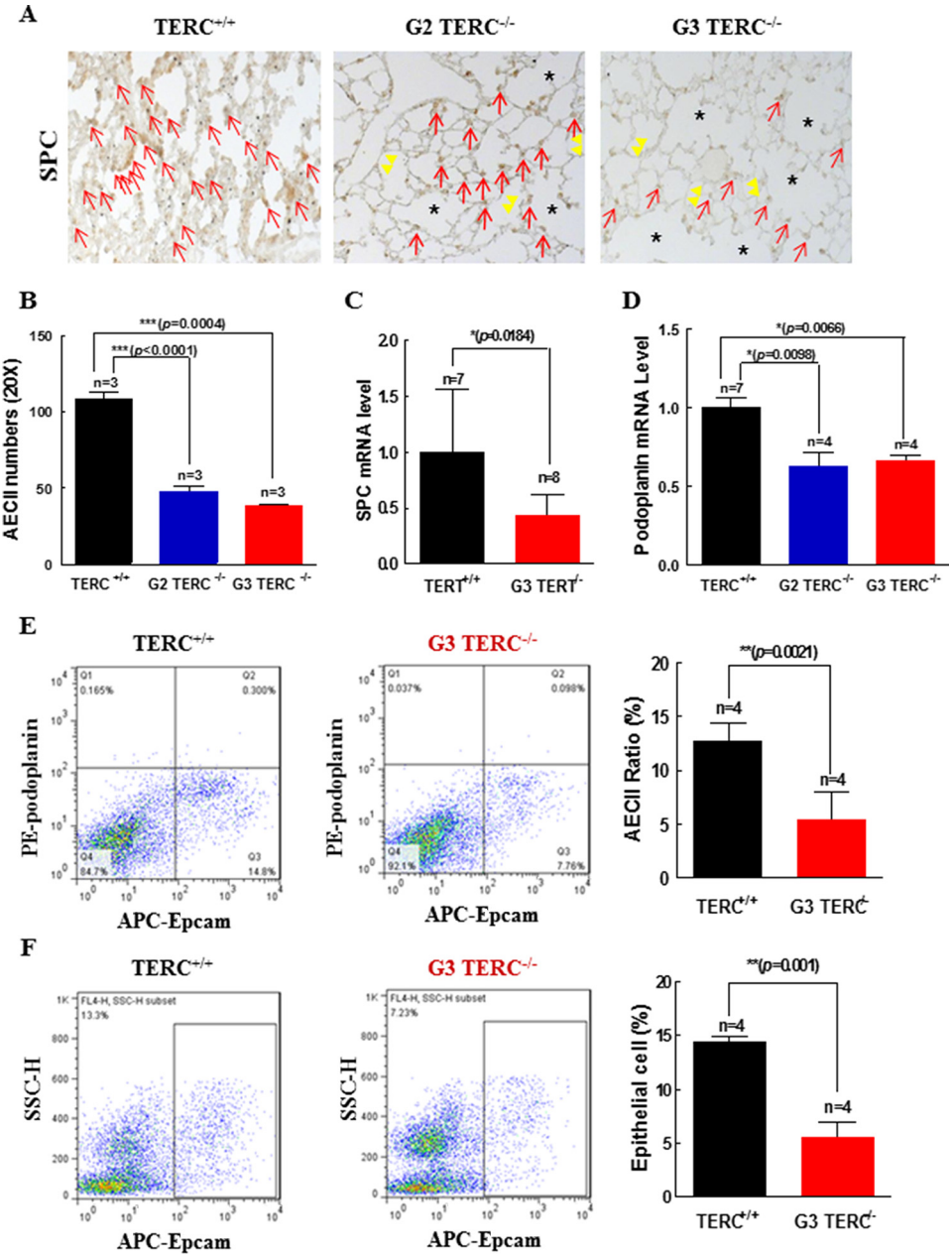

FIGURE 2. **TERC or TERT deficiency induced alveolar epithelial cell replicative senescence.** *A*, SPC-positive staining of AECII in TERC-null mice by immunohistochemistry. *Red arrows*, SPC-positive staining; *double yellow arrowheads*, thin alveolar walls; *asterisks*, alveolar sacs. *B*, quantitation of AECII on the pulmonary sections from WT, G2, and G3 TERC-null mice. Data are the mean ± S.D. (*error bars*) from three animals. *C*, SPC mRNA expression in AECII from TERT-null mice. Data are the mean ± S.E. (*error bars*) ($n = 8$). *D*, podoplanin mRNA expression in alveolar epithelial type I cells from TERC-null mice. Data are the mean ± S.E. ($n = 4$). *E*, AECII in the lung of G3 TERC-null mice by flow cytometry labeled with APC-EpCAM and PE-podoplanin. The *left* and *middle panels* are representative of AECII sorting, and the *right bar graph* shows the pooled data (mean ± S.E.) from four animals. *F*, total alveolar epithelial cells in the lung of G3 TERC-null mice were labeled with APC-EpCAM and analyzed by flow cytometry. The *left* and *middle panels* are representative of cell sorting, and the *right bar graph* shows the pooled data (mean ± S.E.) from four animals.

decreased alveolar numbers (Fig. 1*C*), detection of alveolar fusion and formation of alveolar sacs (Fig. 1*D*), and increased total alveolar surface areas (Fig. 1, *A*, *B*, and *E*), indicative of pulmonary epithelial aging and atrophy. β-Gal staining for cellular senescence was markedly increased in G3 TERC-null and G3 TERT-null lung sections compared with control (Fig. 1, *A* and *B*). Upon examination of the alveolar stem cell AECII population that express SPC and telomerase activity (25, 32, 37), we found that senescent β-gal-positive cells were significantly increased among the AECII population from G2 TERC-null and G3 TERT-null animals by flow-β-gal analysis (Fig. 1, *F*–*H*). Furthermore, SPC-positive cells were significantly reduced in association with thinner alveolar walls and increased alveolar fusions, resulting in alveolar sacs in the mice of both the second and third generations lacking TERC (Fig. 2, *A* and *B*). Gene expression analysis also showed reduced SPC mRNA in G3 $TERT^{-/-}$ lung to 45% of that in wild type controls (Fig. 2*C*). In addition to a compromised AECII population, the reduction in podoplanin gene expression in both G2 and G3 TERC-null mice to about 60% of that in the wild type controls (Fig. 2*D*) suggested a possible decline of the AECI population as well. To further verify the altered AECII populations in G3 TERC-null

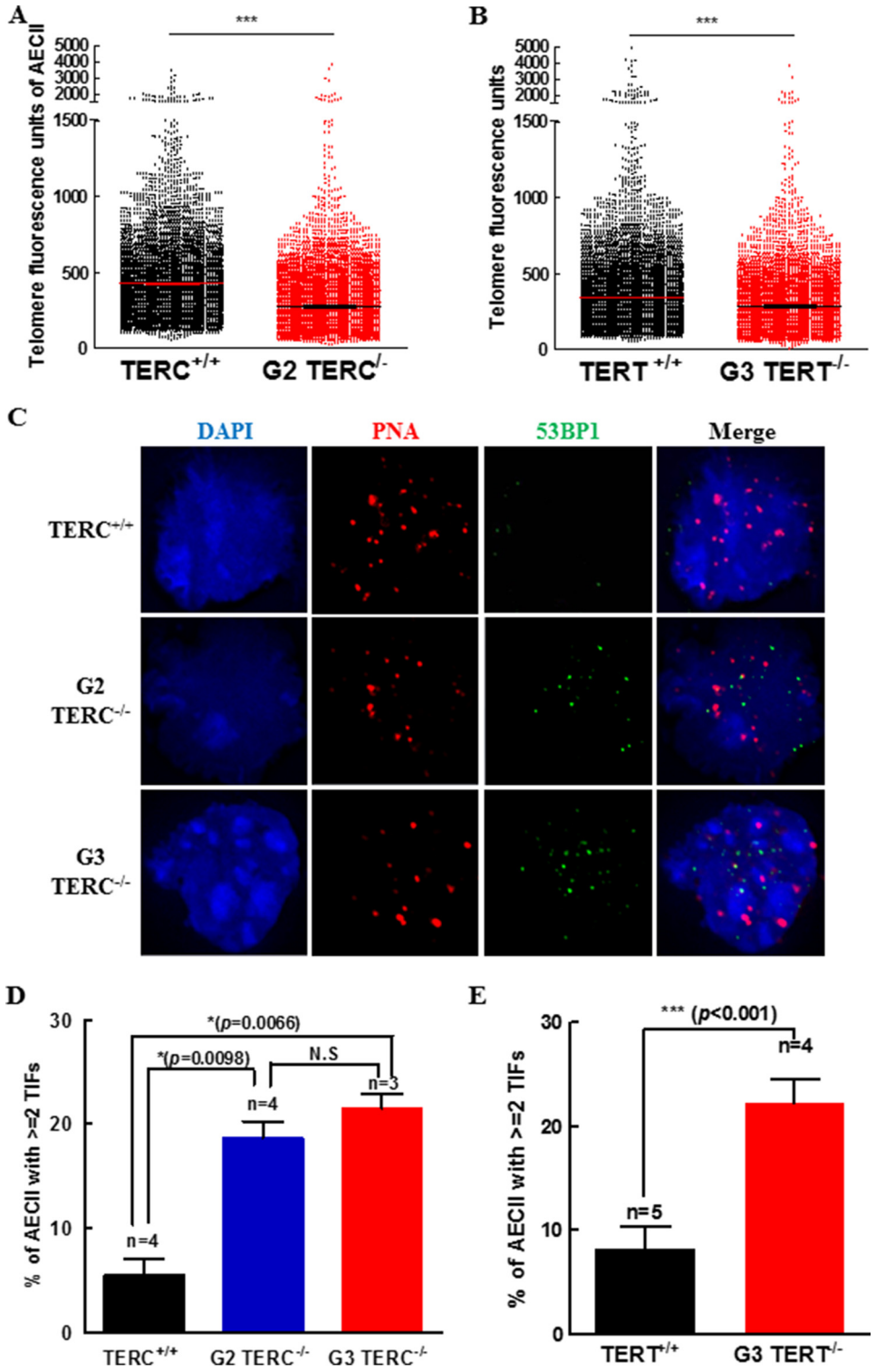

FIGURE 3. **Telomerase deficiency induced telomere shortening and TIFs in isolated AECII population.** *A* and *B*, distributions of telomere length in AECII determined by quantitative FISH and expressed as mean telomere fluorescence of each isolated AECII. *C*, micrographs of peptide nucleic acid probe-labeled telomeres, 53BP1 antibody-labeled damaged DNA, and co-localized telomere and 53BP1 foci. *D* and *E*, mean counts for isolated AECII with each cell containing more than two TIFs. *Error bars*, S.E.

mice, AECII were isolated from the mouse pulmonary tissues using fluorescence-activated cell sorting (FACS) analysis for immunoreactive EpCAM labeling of the epithelial compartment and podoplanin unlabeling of AECII. AECII were reduced to ~45% in G3 TERC$^{-/-}$ mice in comparison with age- and sex-matched wild type (WT) mice (Fig. 2*E*). The total EpCAM-positive cells were reduced to about 40% (Fig. 2*F*).

Consistent with replicative senescence, (Fig. 2), deletion of either G2 TERC or G3 TERT resulted in significant shortening of telomere length in AECII (Fig. 3, *A* and *B*). Moreover, we

noted a significant rise in TIFs in the G2 TERC- or G3 TERT-deficient lung sections (Fig. 3, *C–E*), consistent with telomere DNA damage response (DDR). In association with shortened telomere length and telomere DDR in the AECII (Figs. 3 and 4A), p15 and p21 were both increased significantly in the lungs of G3 TERC$^{-/-}$ mice compared with the control samples from WT mice (Fig. 4, *B* and *C*), and p15, p16, and p21 were increased significantly in the lungs of G3 TERT$^{-/-}$ mice (Fig. 4, *D–F*). Examination of p16 in the AECII of mouse lung sections showed that the levels of immunoreactive p16 were increased by more than 3-fold in the G3 TERT$^{-/-}$ mice compared with the WT animals (Fig. 4*G*). Moreover, we analyzed the levels of heterochromatin protein 1γ (HP1γ), a marker for senescence-associated heterochromatin foci, and found that immunoreactive HP1γ was also markedly increased, with the level of HP1γ in G3 TERT$^{-/-}$ AECII being more than 2.5 times that in WT control animals (Fig. 4*H*) and the level of HP1γ in TERC$^{-/-}$ AECII being more than 4 times that in WT control (Fig. 5*A*). Thus, these data indicated that loss of telomerase resulted in AECII replicative senescence and premature pulmonary aging in mice.

Deficiency in TERC Induced the Increases in α-SMA and Col1α1 Gene Expressions in the Lungs—The lung tissues of G3 TERC$^{-/-}$ mice showed no apparent phenotype of fibrosis, consistent with previous findings (26, 27, 30, 38). However, examinations for gene expressions of the fibrotic markers, α-SMA and Col1α1, in the lungs of 3-month-old G3 TERC$^{-/-}$ mice revealed that both α-SMA and Col1α1 were significantly increased in the G3 TERC$^{-/-}$ mice compared with control animals (Fig. 5, *C–H*). Staining for immunoreactive α-SMA showed that significant levels of α-SMA were detectable in the pulmonary interstitium of the G3 TERC$^{-/-}$ mice, without co-localization with AECII marker SPC (Fig. 5, *C* and *D*). To show the induced gene expression of α-SMA in the lungs of TERC$^{-/-}$ mice, α-SMA mRNA was measured by real-time quantitative PCR in G2 and G3 TERC$^{-/-}$ mice and controls. As shown in Fig. 5*E*, the level of α-SMA gene expression was increased significantly in the lungs of both G2 and G3 mice lacking TERC, in comparison with WT controls. Whereas the level of α-SMA mRNA in the lungs of G2 TERC$^{-/-}$ mice was greater than that in the WT controls (1.24 *versus* 1.0, $p = 0.0267$, $n = 4$), the level of α-SMA mRNA in the lungs of G3 TERC$^{-/-}$ mice was higher than that in both WT controls (1.54 *versus* 1.0, $p = 0.0016$, $n = 5$) and G2 TERC$^{-/-}$ mice (1.54 *versus* 1.24, $p = 0.0385$) (Fig. 5, *C–E*). Western blotting confirmed a 1.5-fold increase in α-SMA in association with decreased SPC and increased p53 in the lung tissue of G2 TERC-null mice (Fig. 5*F*).

In addition to α-SMA, we also examined the fibrotic marker Col1α1 in the lungs of G3 TERC$^{-/-}$ mice. We found that the immunoreactive Col1α1 was detected at significant levels in the pulmonary tissues of WT mice, but the levels in the lungs of G3 TERC$^{-/-}$ mice were significantly greater than that in WT animals (303 *versus* 393 arbitrary units, $p < 0.001$, $n = 3$) (Fig. 5, *G* and *H*). These data suggest that disruption of either TERC or TERT with shortened telomeres and telomere DDR incurred an elevation of myofibroblast activity in the pulmonary interstitium.

Loss of Telomerase Caused Altered Levels of Cytokines and Growth Factors in the Bronchoalveolar Lavage Fluids and Pulmonary Tissues—Because of the enhanced expression of α-SMA and Col1α1 in the pulmonary interstitium of G3 TERC-null mice, to shed light on a potential mechanism of the participation of TGF-β (39, 40), we measured gene expressions of TGF-β and its receptors. However, we observed significant decreases in TGF-β1, TGFβRII, and TGFβRI receptors (Fig. 6, *A–C*) but an increase in BMPRIb receptor despite unaltered BMPRII and BMPRIa levels in G3 TERT$^{-/-}$ mice compared with WT (Fig. 6, *D–F*). Consistently, we found that there was a significant decrease in immunoreactive TGF-β1 in response to lipopolysaccharide (LPS) in the BAL fluids of G3 TERC$^{-/-}$ mice (Fig. 6*G*). In contrast, there were marked increases in immunoreactive IL-6 and CXCL15 in both TERC$^{-/-}$ and TERT$^{-/-}$ mice, with IL-6 being more than 7-fold and CXCL15 more than 10-fold higher than in control mice (Fig. 6, *H–K*).

In the G2 TERC$^{-/-}$ mouse lungs, we observed significant increases in the gene expressions of a number of cytokines: IL-1β (2.6-fold), IL-2 (1.9-fold), IL-6 (0.4-fold), CXCL15 (0.5-fold), CCL2 (2.2-fold), TNF-α (1.6-fold), and IL-10 (1.5-fold) (Fig. 7*A*). Similarly, in the G2 TERT$^{-/-}$ mouse lungs, there were dramatic increases in IL-1α (2.5-fold), IL-1β (3-fold), IL-2 (9.6-fold), IL-6 (2.9-fold), CXCL15 (3-fold), CCL2 (16-fold), TNF-α (3-fold), and IL-10 (4.5-fold) (Fig. 7*B*). These data demonstrated a striking phenotype of AECII- and pulmonary-specific senescence-associated secretory phenotype (SASP) in both TERC$^{-/-}$ and TERT$^{-/-}$ lungs.

Given the marked increases in inflammatory cytokines in the lungs of TERC$^{-/-}$ and TERT$^{-/-}$ mice, we determined the potential inflammatory cell responses in the lungs of the TERC$^{-/-}$ mice. Consistent with increased chemotactic effects of the secreted cytokines, increased cell populations positive for CD45 and CD16/CD32 but negative for EpCAM were observed in the lungs of G3 TERC$^{-/-}$ mice compared with WT controls (Fig. 8, *A* and *B*). The average number of CD45-positive cells in G3 TERC$^{-/-}$ lungs appeared to be double that in the lungs of WT controls (Fig. 8*A*), and CD16/CD32-positive cells were also double the control levels (Fig. 8*B*). Furthermore, there was a significant increase in a cell population positive for CD11b (Aka CR3, iC3b receptor) (Fig. 8*C*). It is important to note that CD11b is an active constituent of the innate immune response of the host, with functions of a pattern recognition receptor recognized by ligands including fibrinogen, Factor X, intercellular adhesion molecule 1 (ICAM-1), *Saccharomyces cerevisiae*, *Staphylococcus epidermidis*, *Hislasma capsulatum* by opsonizing phagocytosis, neutrophil aggregation, adhesion, and chemotaxis (41, 42). In the same pulmonary tissues of G3 TERC$^{-/-}$ mice, however, we found no significant change in the numbers of macrophage, NK cells, or dendritic cells (Fig. 8, *D–F*). No significant changes were found in B cells (17.78 ± 4.69% *versus* 16.6 ± 5.75%, $n = 4$, $p > 0.05$), CD4$^+$ T cells (5.65 ± 0.9083% *versus* 5.825 ± 0.3902%, $n = 4$, $p > 0.05$), or CD8$^+$ T cells (5.2 ± 1.004% *versus* 5.775 ± 0.5662%, $n = 4$, $p > 0.05$). Taken together, these data are suggestive of a telomere shortening-induced pulmonary atypical phenotype of low-grade inflammatory processes in association with alveolar stem cell replication senescence.

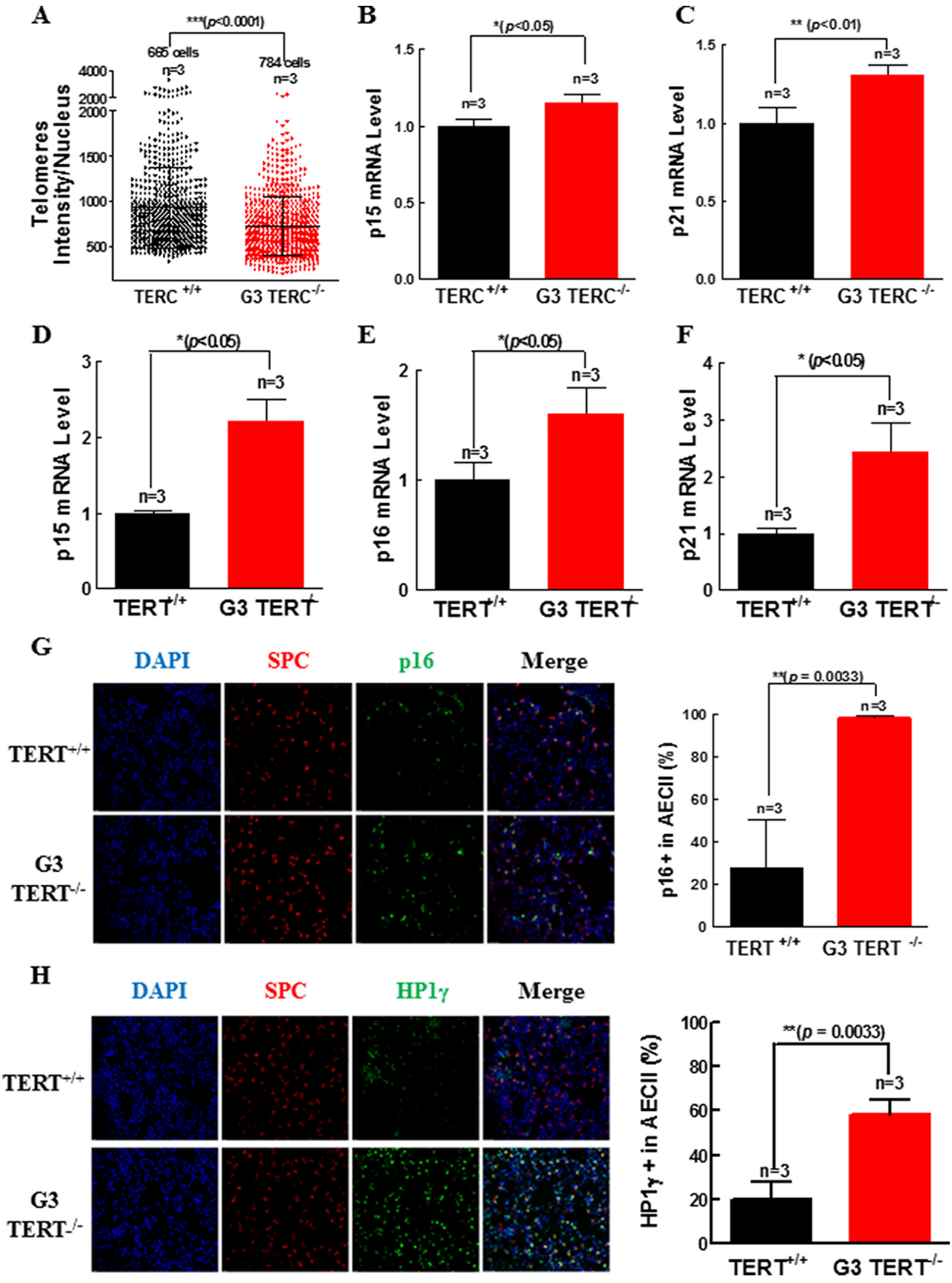
A
***(p<0.0001)
665 cells
n=3
784 cells
n=3
Telomeres Intensity/Nucleus
4000
2000
2000
1500
1000
500
TERC +/+
G3 TERC -/-
B
*(p<0.05)
p15 mRNA Level
1.5
1.0
0.5
0.0
n=3
n=3
TERC +/+
G3 TERC -/-
C
** (p<0.01)
p21 mRNA Level
1.5
1.0
0.5
0.0
n=3
n=3
TERC +/+
G3 TERC -/-
D
*(p<0.05)
p15 mRNA Level
3
2
1
0
n=3
n=3
TERT +/+
G3 TERT -/-
E
*(p<0.05)
p16 mRNA Level
2
1
0
n=3
n=3
TERT +/+
G3 TERT -/-
F
* (p<0.05)
p21 mRNA Level
4
3
2
1
0
n=3
n=3
TERT +/+
G3 TERT -/-
G
DAPI
SPC
p16
Merge
TERT+/+
G3 TERT-/-
**(p = 0.0033)
p16+ in AECII (%)
100
80
60
40
20
0
n=3
n=3
TERT +/+
G3 TERT -/-
H
DAPI
SPC
HP1γ
Merge
TERT+/+
G3 TERT-/-
**(p = 0.0033)
HP1γ + in AECII (%)
100
80
60
40
20
0
n=3
n=3
TERT+/+
G3 TERT-/-

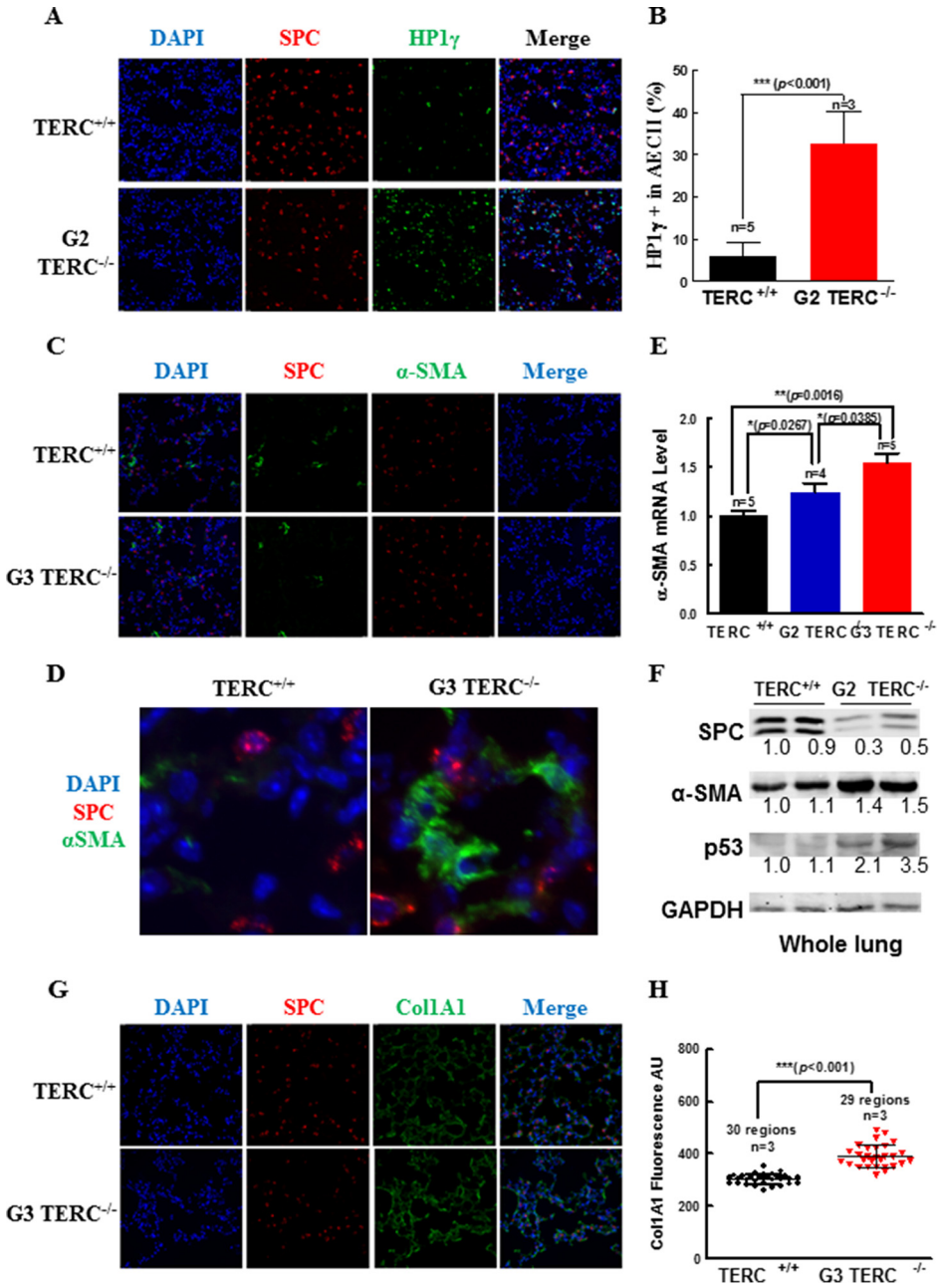

FIGURE 5. **TERC deficiency induced increases of α-SMA and Col1A1 gene expressions in pulmonary AECII.** *A* and *B*, HP1γ and SPC staining in the pulmonary sections from G2 TERC-null mice, with representative micrographs (*A*) and the quantitative data (*B*) (mean ± S.D.) of 3–5 animals. *C* and *D*, α-SMA expression in lung tissue of TERC-null mice detected by immunofluorescence staining using specific antibodies. Enlarged images of WT and TERC-null are shown in *D*. *E*, the α-SMA mRNA levels were measured by quantitative real-time PCR from TERC-null mice lungs. Data are the mean ± S.E. (*error bars*) from at least five animals. *F*, Western blotting assessment of SPC, α-SMA, and p53 immunoreactivities in the lung tissues of duplicate WT and G2 TERC-null mice. *G* and *H*, Col1A1 expression in the lung tissues of TERC-null mice was measured by immunofluorescence staining using specific antibodies. Relative quantification of Col1A1 immunoreactivity was analyzed by Softworx software (*D*). Data are the mean ± S.D. (*error bars*) from three representative experiments. Representative images are shown in *E*.

Telomerase Deficiency-induced Cell Senescence Did Not Cause Altered Gene Expression of Proinflammatory Cytokines in AECII—To determine whether senescent AECII contributed the markedly increased proinflammatory cytokines, we assessed the gene expression levels of several key proinflammatory cytokine between WT, G2 TERC, and G3 TERT-null mice. As shown in Fig. 9, *A* and *B*, whereas the gene expression of α-SMA and SPC did not differ between WT and G2 TERC KO

FIGURE 4. **Shortening of telomeres and increases in p15, p16, and p21 genes in telomerase-deficient lungs.** *A*, quantitative FISH experiment result for isolated AECII from G3 TERC-null mice. The telomere length is represented by fluorescence intensity in scatter plot style. *B* and *C*, the mRNA levels of p15 (*B*) and p21 (*C*) were determined by quantitative real-time PCR from three WT or G3 TERC-null animals as indicated. *D–F*, the mRNA levels of p15 (*D*), p16 (*E*), and p21 (*F*) were determined by quantitative real-time PCR from three WT or G3 TERT-null animals as indicated. *G*, P16 and SPC expression by immunostaining on pulmonary sections from G3 TERT-null mice. The *left panels* are representative micrographs, and the *right bar graph* shows the quantitative data (mean ± S.D. (*error bars*)) of three experiments. *H*, HP1γ and SPC staining on pulmonary sections from G3 TERT-null mice using specific antibodies. The *left panels* are representative micrographs, and the *right bar graph* shows the quantitative data (mean ± S.D.) of three experiments.

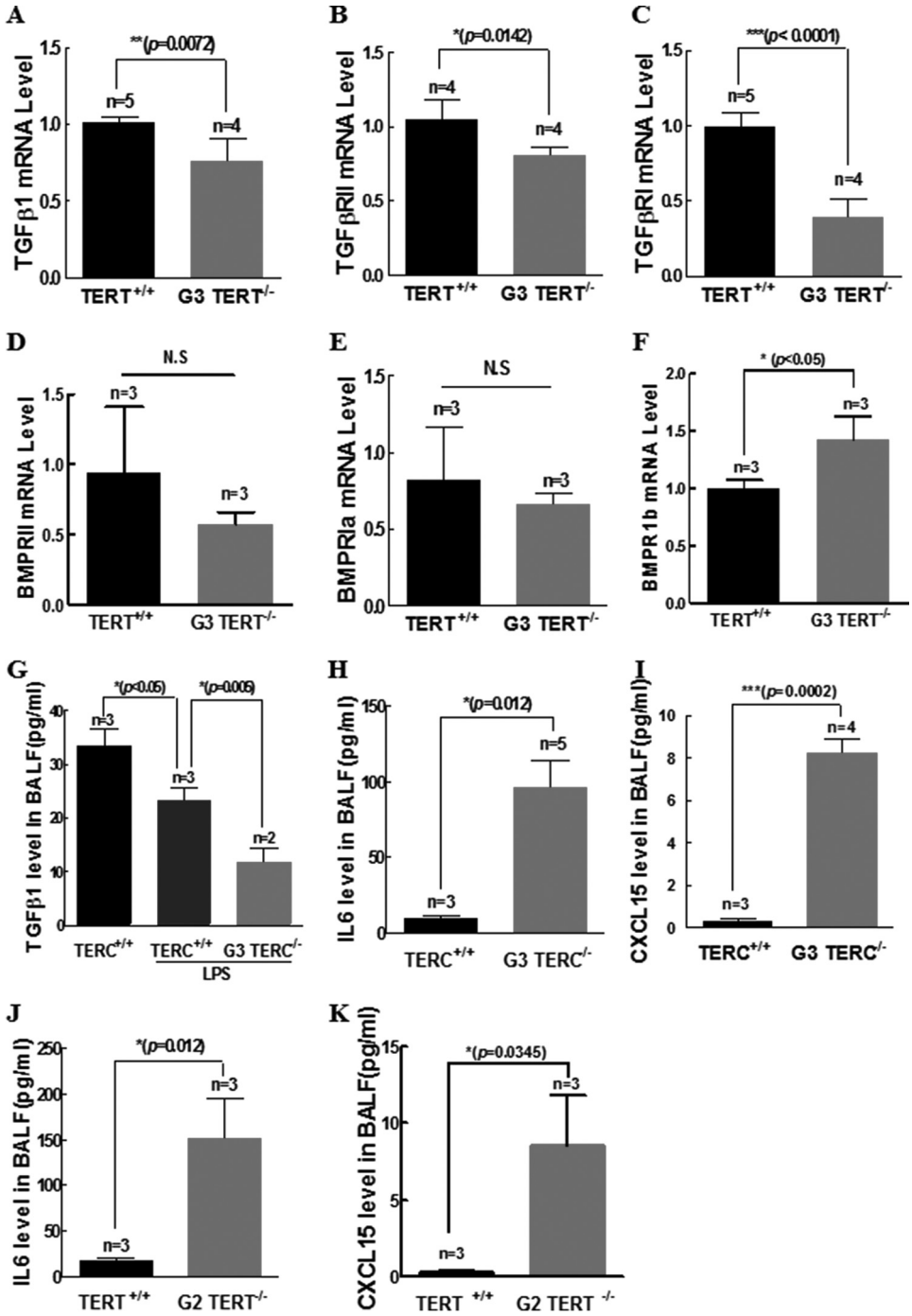

FIGURE 6. **TERC or TERT deficiency resulted in reduced gene expression of TGF-β1 and canonical receptors in pulmonary tissues.** *A–C*, the mRNA levels of TGF-β1 (*A*), TGFβRII (*B*), and TGFβRI (*C*) were determined by quantitative real-time PCR from at least four animals, as indicated. *D–F*, the mRNA levels of BMPRII (*D*), BMPRIa (*E*), and BMPRIb (*F*) were determined by quantitative real-time PCR from at least four animals, as indicated. *G*, TGFβ1 levels detected by ELISA using specific antibodies from BAL fluid of TERC-null mice. *H* and *I*, IL-6 and CXCL15 levels measured by ELISA from BAL fluid of TERC-null mice. *J* and *K*, IL-6 and CXCL15 levels measured by ELISA from BAL fluid of TERT-null mice. All data are the mean ± S.E. (*error bars*) of multiple representative experiments.

AECII (Fig. 9, *A* and *B*), isolated AECII from G2 TERC- and G3 TERT-null animals had significantly increased gene expression of p15 and p21 and decreased gene expression of Ki67 in comparison with control, consistent with telomerase deficiency-induced AECII senescence. However, the gene expression of IL-1α, IL-1β, IL-6, CXCL15, IL-10, TNF-α, TGF-β, TGFβRII, TGFβRI, BMPRII, and BMPRI was not changed in AECII from G2 TERC or G3 TERT-null animals compared with control (Fig. 9, *C* and *D*). These data suggest that the markedly increased proinflammatory cytokines in the TERC- or TERT-deficient lungs are largely from other unidentified cells rather than from senescent AECII.

Discussion

Gene mutations of *TERC* and *TERT* cause telomere shortening, which is significantly associated with the clinical manifestations and pathologies of dyskeratosis congenita, bone marrow failure, and pulmonary fibrosis, among others (25–30). A causal

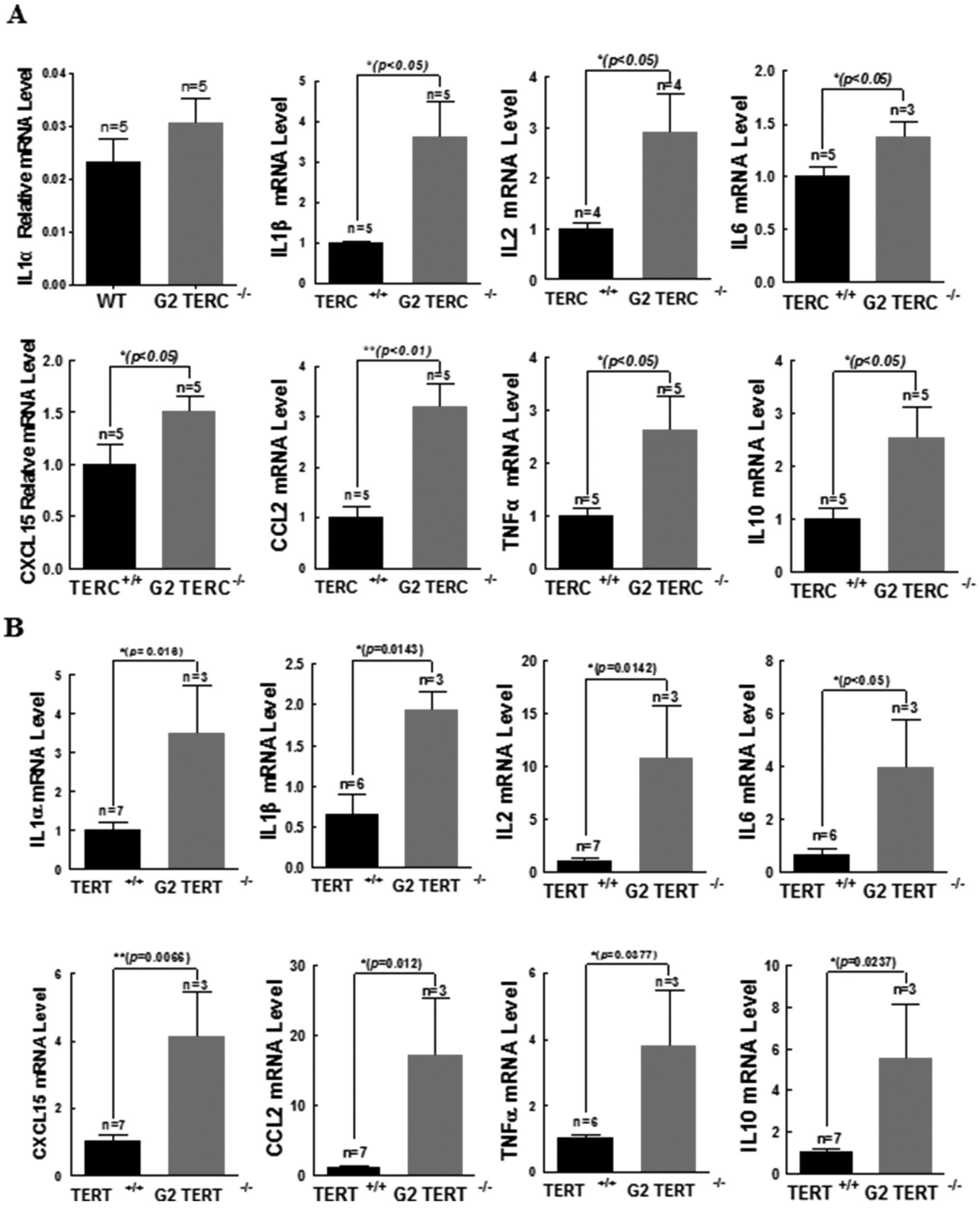

FIGURE 7. **TERC or TERT deficiency induced significant disorders of cytokines and growth factors in the pulmonary tissues.** *A*, IL-1α, IL-1β, IL-2, IL-6, CXCL15, CCL2, TNF-α, and IL-10 mRNA levels were detected in TERC-null mice lungs by quantitative PCR. *B*, IL-1α, IL-1β, IL-2, IL-6, CXCL15, CCL2, TNF-α, and IL-10 mRNA levels were detected in TERT-null mice lungs by quantitative PCR. All data are the mean $\pm$ S.E. (*error bars*) of multiple similar experiments. Statistical *p* values are as indicated.

role of either TERC or TERT deficiency has been established in mouse models, including phenotypes resembling dyskeratosis congenita and bone marrow failure (23). To understand the cellular mechanisms underlying telomerase gene mutation-induced lung injuries and to determine whether AECII undergo replicative senescence, we examined various cellular markers,

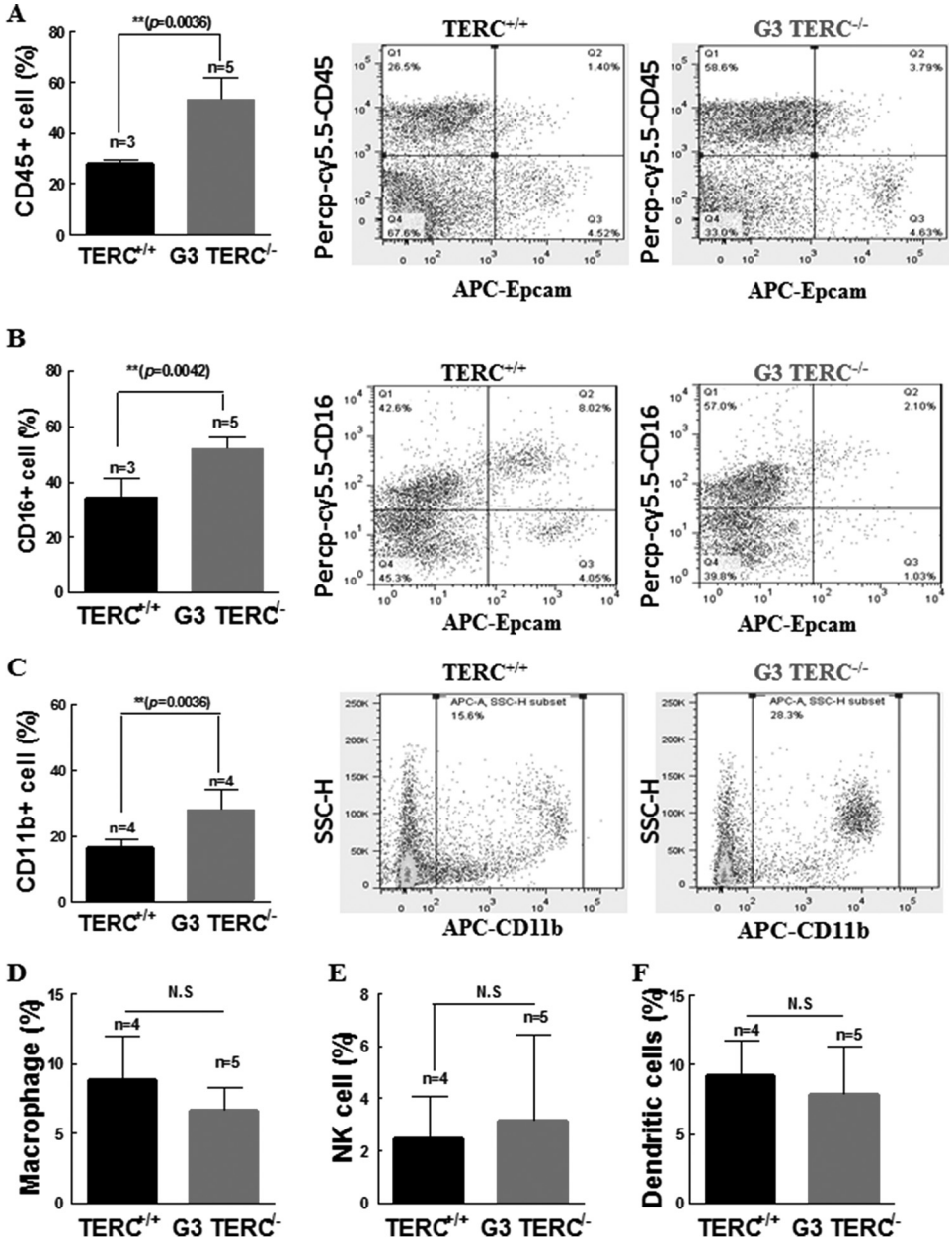

FIGURE 8. **TERC deficiency resulted in inflammatory cell infiltration in pulmonary tissues.** *A*, TERC deficiency induced increases in CD45-positive mononuclear cells. The *left bar graph* shows summarized data presented as the mean ± S.D. (*error bars*) from three flow cytometric analyses. The *middle* and *right panels* are representative plots of cell distributions labeled by Percp-cy5.5-CD45 but not by EpCAM. *B*, TERC deficiency induced increases in CD16/32-positive mononuclear cells. The *left bar graph* shows summarized data presented as mean ± S.D. from at least three animals. The *middle* and *right panels* are representative plots of cell distributions labeled by APC-CD11b. *C*, TERC deficiency induced increases in CD11b-positive mononuclear cells. The *left bar graph* shows summarized data presented as mean ± S.D. from at least three animals. The *middle* and *right panels* are representative plots of cell distributions labeled by FITC-F1/80, PE-NK1.1, and APC-CD11c (*D–F*). TERC deficiency resulted in no changes in the ratios of macrophages (*D*), NK cells (*E*), or dendritic cells (*F*) by flow cytometry.

including extracellular factors such as TGF-β, in SPC-positive cell populations in TERC$^{-/-}$ and TERT$^{-/-}$ mice. Our findings that a significant population of AECII undergoes replicative senescence, that increased α-SMA and Col1α1 expression (markers of myofibroblast differentiation) occurs in the telomerase-deficient pulmonary interstitium, and that a marked increase in proinflammatory cytokines in the telomerase-deficient lung tissues, with a significant spillover into the BAL fluids, together with recruitment of inflammatory cells in the innate immune response, may constitute a signature of chronic low-grade inflammation incurred by telomerase deficiency and telomere damage.

Previous studies have indicated that telomerase activity is operative in normal AECII (25, 32, 37) and is stimulated by silica inhalation and bleomycin instillation, which causes pulmonary fibrosis in rodents (43, 44). Whereas disruption of *Terc* or *Tert* leads to inhibition of telomerase activity and shortening of telomeres in mouse AECII (25, 45), the damaging effect of telomere ablations on cellular homeostasis remains to be determined. We demonstrate in the present study that disruption of

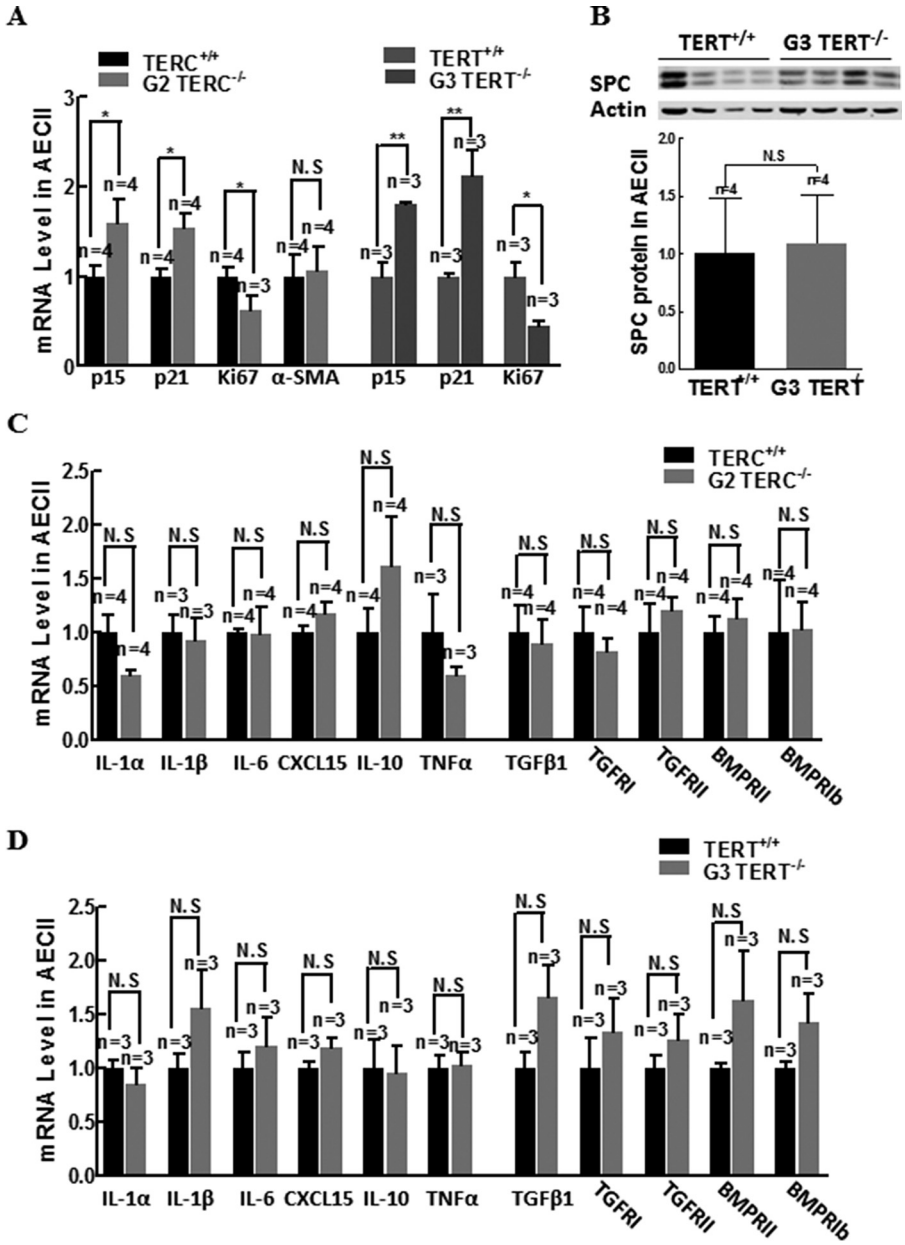

FIGURE 9. **Characterization of AECII gene expression of proliferation markers, proinflammatory cytokines, TGF-β1, and receptors.** *A*, transcriptional levels of proliferation marker, p15, p21, and Ki67 mRNAs in isolated AECII from telomerase wild type and deficient mouse lungs by quantitative PCR. *B*, SPC protein expression in isolated AECII measured by Western blotting and analyzed with semiquantification. *C*, transcriptional levels of IL and TGF-β family mRNAs in isolated AECII from G2 TERC-null mice lungs. *D*, transcriptional levels of IL and TGF-β family mRNAs in isolated AECII from G3 TERT-null mice lungs. *Error bars*, S.E.; *N.S*, not significant.

Terc or *Tert* initiates telomere DDR with decreased telomere length; increased TIFs; increased p15, p16, and p21; and inductions of AECII replicative senescence characteristic of reduced total numbers of AECII and increased populations of AECII positive for HP1γ and β-gal staining. In addition, we demonstrate pulmonary premature aging in either TERC- or TERT-deficient mice, consistent with previous studies indicating that TERC deficiency results in decreased AECII, in association with alveolar wall thinning and air sac formation (25). It is thus possible that lack of telomerase support in telomere maintenance compromises AECII proliferative potential, resulting in disrepairs of alveolar epithelium. Consistently, we show a 60% reduction in total epithelial cell compartment positive for EpCAM staining in the absence of TERC. Although the mechanisms mediating AECI senescence are intriguing, our data lend support to the recent discoveries that telomerase deficiency renders pulmonary tissues susceptible to damage caused by cigarette smoke, potentially underpinning emphysema with or without pulmonary fibrosis (27, 46, 47), thus indicating that telomerase is required for AECII and is responsible for AECII renewal and proliferation in adult animal pulmonary interstitium (48, 49).

The subpopulations of AECII have been demonstrated in both humans and mice. Analysis of E-cadherin low and high AECII subpopulations demonstrates that E-cadherin low AECII represent a major population of AECII positive for

telomerase activity, proliferative, and resistant to damage, whereas E-cadherin high AECII is a minor population that is negative for telomerase and quiescent in mouse lungs (32). In humans, by contrast, a significant minor subpopulation of AECII is positive for telomerase, and a large population is telomerase-negative in the normal areas of lungs, but low or negative telomerase correlates with high apoptotic signals in AECII of IPF (50). The difference in the size of mouse *versus* human AECII telomerase-positive and -negative subpopulations is interesting, indicating a limitation of the present study using mouse models to recapitulate the phenotypes of IPF. Further investigations are required to characterize additional lesions of genetic and environmental factors in and beyond AECII subpopulations in different species. Nevertheless, our findings that more than half of the retained AECII population in telomerase-deficient lungs undergoes senescence are consistent with the notion that a major subtype of AECII is telomerase-positive, with telomere homeostasis playing a key role in regulating AECII proliferative and differentiating potentials in mice. Withdrawal of telomerase activity plays a large part in alveolar stem cell replicative senescence, pulmonary aging, and disordered cellular conditions, as seen in emphysema and IPF (32, 47, 48, 51).

Recent studies also indicate that regulation of AECII by extracellular signaling predominantly dictates AECII response to injury signals and that only about 1% of mature AECII divide intermittently, with an approximately 40-day doubling time, supporting an overall renewal rate of 7% of alveoli/year (49). Injuries to the AECI population, together with EGF receptor activation, induce AECII broad stem cell functions (49). Whereas activation of the Ras-ERK pathway stimulates proliferation (49) and inhibits differentiation (52) of AECII, inhibition of the Ras-ERK pathway is essential for TGF-β1-induced AECII differentiation (52). Interestingly, we and others showed previously that whereas mitogens up-regulate telomerase activity by Ets transcriptional activation of the *TERT* gene (53, 54), TGF-β family members down-regulate telomerase activity by Smad3 transcriptional repression of *TERT* in epithelial cell lines (55–57). These data together suggest that the EGF-Ets and TGF-β-Smad3 pathways regulate the *TERT* gene and proliferative potential of AECII in a reciprocally opposing manner. However, in opposition to our hypothesis that TGF-β is stimulated to participate in telomere dysfunction-induced epithelial to mesenchymal transition, we note in our present study that TGF-β1 and its receptors are down-regulated (rather than up-regulated) in the lungs of TERT knock-out mice. Given that TGF-β is implicated in autocrine regulation of telomerase (57), our findings of down-regulated TGF-β and its canonical receptors are consistent with a compensatory negative feedback on the *Tgf-β* and *Tgfβri* genes. Noting the unexpected findings of low TGF-β signaling from the present study, several questions remain to be addressed, including whether cytokine regulation confers stemness upon AECII at least in part by mechanisms dependent on regulated telomerase maintenance of telomere functionality.

TGF-β is a key player in antagonizing AECII proliferation but stimulating AECII differentiation (40, 58–64). To date, it is still unclear which transcriptional targets downstream of TGF-β signaling mediate AECII differentiation and whether TGF-β-induced Smad3-mediated telomerase down-regulation plays a part in suppressing AECII proliferation and allowing AECII to undergo differentiation. In the absence of telomerase, although both TGF-β and its receptor are down-regulated, we found increased α-SMA and Col1α1 in the telomerase-deficient lungs but not in AECII (Fig. 5). Previous studies showed increased expression of α-SMA in AECII as a marker of AECII undergoing the gene expression involved in myofibroblasts by epithelial to mesenchymal transition (52, 61, 65). Because anomalous expression of α-SMA and Col1α1 in AECII is among the features of AECII trans-differentiation to myofibroblasts and is suggestive of a fibrotic lesion of pulmonary fibrosis (61, 65), further investigations are required to characterize the regulatory mechanisms underlying the limited tempo-spatial processes and scales of AECII trans-differentiation triggered by telomere dysfunction. Recent studies have shown that TGF-β stimulates α-SMA gene expression through Smad3 interaction with β-catenin on the α-SMA gene promoter in AECII (66). In addition, TGF-β activates the TRPV4 (transient receptor potential vanilloid 4) channels and actin polymerization, resulting in the formation and nuclear translocation of the myocardin-related transcription factor·serum response factor complex and the subsequent stimulation of the α-SMA gene transcription (67). In the face of telomere dysfunction and down-regulated TGF-β signaling in this study, it is conceivable that in addition to the accelerated cellular senescence prompted by telomere DDR, a second hit of genetic or environmental insults may be accountable for full development of IPF-like phenotypes (68, 69).

As demonstrated in the current study, inflammatory cytokines are markedly increased in the lungs of mice deficient in either TERC or TERT (Figs. 7 and 8). The concentrations of IL-6, CXCL15, and TNF-α in the pulmonary parenchyma are increased severalfold with a significant spillover into the BAL fluids in telomerase-deficient mice. These findings of telomere dysfunction-caused SASP profiles of altered cytokines and growth factors in the mouse pulmonary tissues are consistent with persistent telomere DDR in both human and mouse studies (70–72). The findings of markedly increased IL-1α and IL-1β are consistent with their regulatory roles in increased IL-6 and IL-8 (72). Although we have confirmed the previous findings that IL-10 is increased along with TNF-α in the settings of telomere DDR (73), we also found that increased CCL2 is significantly involved in the microenvironment of telomere-induced AECII senescence, probably with a fundamental role in the recruitment of NK cells (74). In an attempt to address a link between AECII senescence and proinflammatory cytokine rise in the lungs of telomerase-deficient mice, we examined whether senescent AECII contributed the increase of proinflammatory cytokines with increased gene expression in the senescent AECII. Our finding that telomerase deficiency-induced senescent AECII had no significant change in proinflammatory cytokine gene expression suggests that senescent AECII interact with other cells in eliciting increased proinflammatory cytokines.

Although the isolated senescent AECII showed no significant rise in certain proinflammatory cytokine gene expressions (Fig.

9), the possibility cannot be ruled out that senescent cells release an unidentified signal in SASP that engages another cell type to provoke proinflammatory cytokine storms. SASP may represent an initial step to signal the intermediate mediators of the sterile senescence-associated low-grade inflammation in aging-related disorders. Consistently, there is a large heterogeneous population of mononuclear inflammatory cells that are positive for CD45 and/or CD16/32 in the TERC-deficient lungs. Together, these data reveal a novel phenotype characteristic of telomere-induced, stem cell senescence-associated, low-grade inflammation (SALI). Because telomere DDR triggers the permanent exit of the cell cycle in the stem cells deficient in telomerase, SALI may represent a potential mechanism by which other cells of the same and differentiated types, such as AECI, undergo cellular senescence. In support of this hypothesis, recent studies have demonstrated that chronic inflammation is sufficient to induce telomere dysfunction and accelerates aging in mice (75). Thus, as a predominant means of eliciting differentiated AECI senescence and accelerating that of AECII, SALI may be both the effect of telomere DDR in some senescent foci and the cause of telomere DDR in other senescent foci, representing a cellular mechanism of the tissue senescence-inducing circuit spreading cellular senescence in pulmonary aging.

In addition to mediating senescence transmission across different senescent foci, SALI may also serve as a pivotal switch in the full development of aging-related disorders by provoking the transitions from cellular senescence to tissue pathologies involving the processes of cell de-differentiation, trans-differentiation, death, immortalization, and transformation. By bridging and mediating the development of tissue pathology, SALI may thus represent a critical window of intervention by molecular targeting in aging-related disease. Although little is known of how telomere-induced SASP (tSASP) and subsequent tSALI are regulated, it is tempting to postulate three possible pathways through which tSASP progresses to tSALI: first, telomere shortening in a particular cell type unchecks the telomere position effect on the transcriptions of the genes encoding inflammatory cytokines and pathogenic factors at different chromosomes, given the recent demonstrations of telomere position effect operation over long distances (76); second, telomere shortening in responsible cells renders epigenetic alterations of heterochromatin formation, resulting in activation of a specific group of gene expressions (77); third, telomere DNA fragments shed off of chromosomes into the extracellular environment serve as damage-associated molecular patterns that perpetuate the tSALI response, by analogy to mitochondrial and mammalian DNA molecules acting as damage-associated molecular patterns (78, 79).

In summary, we demonstrate that telomerase deficiency causes AECII alveolar stem cell telomere shortening and replicative senescence underlying pulmonary aging in mice. We show that telomere shortening not only instigates tSASP of AECII alveolar stem cells, but also drives low-grade inflammation (tSALI) with extensive proinflammatory cytokine spillover and particular inflammatory cell infiltration in pulmonary tissues *in vivo* in mice. The tSASP of AECII stem cells and tSALI may represent crucial steps toward telomerase mutation-associated pathological changes, providing strategies for therapeutic intervention.

Author Contributions—R. C. designed, performed, and analyzed the experiments. K. Z. designed and analyzed the experiments. H. C., X. Z., and J. W. provided technical assistance. J. J., L. L., Y. C., Z. J., D. X., and B. R. G. W. provided technical expertise and contributed the discussions. J. P. L. conceived the study; designed, analyzed, and supervised the experiments; and wrote the paper. All authors reviewed the results and approved the final version of the manuscript.

Acknowledgments—We thank Dr. Yie Liu for supplying the TERT$^{-/-}$ mice and Li Shen for excellent technical support.

References

1. Blackburn, E. H. (2005) Telomeres and telomerase: their mechanisms of action and the effects of altering their functions. *FEBS Lett.* **579,** 859–862
2. Nandakumar, J., and Cech, T. R. (2013) Finding the end: recruitment of telomerase to telomeres. *Nat. Rev. Mol. Cell Biol.* **14,** 69–82
3. Armanios, M. (2013) Telomeres and age-related disease: how telomere biology informs clinical paradigms. *J. Clin. Invest.* **123,** 996–1002
4. Kong, C. M., Lee, X. W., and Wang, X. (2013) Telomere shortening in human diseases. *FEBS J.* **280,** 3180–3193
5. Mitchell, J. R., Wood, E., and Collins, K. (1999) A telomerase component is defective in the human disease dyskeratosis congenita. *Nature* **402,** 551–555
6. Vulliamy, T., Marrone, A., Goldman, F., Dearlove, A., Bessler, M., Mason, P. J., and Dokal, I. (2001) The RNA component of telomerase is mutated in autosomal dominant dyskeratosis congenita. *Nature* **413,** 432–435
7. Vulliamy, T., Marrone, A., Dokal, I., and Mason, P. J. (2002) Association between aplastic anaemia and mutations in telomerase RNA. *Lancet* **359,** 2168–2170
8. Yamaguchi, H., Calado, R. T., Ly, H., Kajigaya, S., Baerlocher, G. M., Chanock, S. J., Lansdorp, P. M., and Young, N. S. (2005) Mutations in *TERT*, the gene for telomerase reverse transcriptase, in aplastic anemia. *N. Engl. J. Med.* **352,** 1413–1424
9. Hartmann, D., Srivastava, U., Thaler, M., Kleinhans, K. N., N'Kontchou, G., Scheffold, A., Bauer, K., Kratzer, R. F., Kloos, N., Katz, S. F., Song, Z., Begus-Nahrmann, Y., Kleger, A., von Figura, G., Strnad, P., Lechel, A., Günes, C., Potthoff, A., Deterding, K., Wedemeyer, H., Ju, Z., Song, G., Xiao, F., Gillen, S., Schrezenmeier, H., Mertens, T., Ziol, M., Friess, H., Jarek, M., Manns, M. P., Beaugrand, M., and Rudolph, K. L. (2011) Telomerase gene mutations are associated with cirrhosis formation. *Hepatology* **53,** 1608–1617
10. Calado, R. T., Brudno, J., Mehta, P., Kovacs, J. J., Wu, C., Zago, M. A., Chanock, S. J., Boyer, T. D., and Young, N. S. (2011) Constitutional telomerase mutations are genetic risk factors for cirrhosis. *Hepatology* **53,** 1600–1607
11. Armanios, M. Y., Chen, J. J., Cogan, J. D., Alder, J. K., Ingersoll, R. G., Markin, C., Lawson, W. E., Xie, M., Vulto, I., Phillips, J. A., 3rd, Lansdorp, P. M., Greider, C. W., and Loyd, J. E. (2007) Telomerase mutations in families with idiopathic pulmonary fibrosis. *N. Engl. J. Med.* **356,** 1317–1326
12. Tsakiri, K. D., Cronkhite, J. T., Kuan, P. J., Xing, C., Raghu, G., Weissler, J. C., Rosenblatt, R. L., Shay, J. W., and Garcia, C. K. (2007) Adult-onset pulmonary fibrosis caused by mutations in telomerase. *Proc. Natl. Acad. Sci. U.S.A.* **104,** 7552–7557
13. Cronkhite, J. T., Xing, C., Raghu, G., Chin, K. M., Torres, F., Rosenblatt, R. L., and Garcia, C. K. (2008) Telomere shortening in familial and sporadic pulmonary fibrosis. *Am. J. Respir. Crit. Care Med.* **178,** 729–737
14. Tsang, A. R., Wyatt, H. D., Ting, N. S., and Beattie, T. L. (2012) hTERT mutations associated with idiopathic pulmonary fibrosis affect telomerase activity, telomere length, and cell growth by distinct mechanisms. *Aging Cell* **11,** 482–490

15. Marrone, A., Sokhal, P., Walne, A., Beswick, R., Kirwan, M., Killick, S., Williams, M., Marsh, J., Vulliamy, T., and Dokal, I. (2007) Functional characterization of novel telomerase RNA (TERC) mutations in patients with diverse clinical and pathological presentations. *Haematologica* **92,** 1013–1020
16. Parry, E. M., Alder, J. K., Qi, X., Chen, J. J., and Armanios, M. (2011) Syndrome complex of bone marrow failure and pulmonary fibrosis predicts germline defects in telomerase. *Blood* **117,** 5607–5611
17. Gansner, J. M., Rosas, I. O., and Ebert, B. L. (2012) Pulmonary fibrosis, bone marrow failure, and telomerase mutation. *N. Engl. J. Med.* **366,** 1551–1553
18. Blasco, M. A., Lee, H. W., Hande, M. P., Samper, E., Lansdorp, P. M., DePinho, R. A., and Greider, C. W. (1997) Telomere shortening and tumor formation by mouse cells lacking telomerase RNA. *Cell* **91,** 25–34
19. Rudolph, K. L., Chang, S., Lee, H. W., Blasco, M., Gottlieb, G. J., Greider, C., and DePinho, R. A. (1999) Longevity, stress response, and cancer in aging telomerase-deficient mice. *Cell* **96,** 701–712
20. Wong, K. K., Maser, R. S., Bachoo, R. M., Menon, J., Carrasco, D. R., Gu, Y., Alt, F. W., and DePinho, R. A. (2003) Telomere dysfunction and Atm deficiency compromises organ homeostasis and accelerates ageing. *Nature* **421,** 643–648
21. Chang, S. (2005) Modeling aging and cancer in the telomerase knockout mouse. *Mutat. Res.* **576,** 39–53
22. He, H., Wang, Y., Guo, X., Ramchandani, S., Ma, J., Shen, M. F., Garcia, D. A., Deng, Y., Multani, A. S., You, M. J., and Chang, S. (2009) Pot1b deletion and telomerase haploinsufficiency in mice initiate an ATR-dependent DNA damage response and elicit phenotypes resembling dyskeratosis congenita. *Mol. Cell. Biol.* **29,** 229–240
23. Strong, M. A., Vidal-Cardenas, S. L., Karim, B., Yu, H., Guo, N., and Greider, C. W. (2011) Phenotypes in mTERT$^{+/-}$ and mTERT$^{-/-}$ mice are due to short telomeres, not telomere-independent functions of telomerase reverse transcriptase. *Mol. Cell. Biol.* **31,** 2369–2379
24. Ju, Z., Jiang, H., Jaworski, M., Rathinam, C., Gompf, A., Klein, C., Trumpp, A., and Rudolph, K. L. (2007) Telomere dysfunction induces environmental alterations limiting hematopoietic stem cell function and engraftment. *Nat. Med.* **13,** 742–747
25. Lee, J., Reddy, R., Barsky, L., Scholes, J., Chen, H., Shi, W., and Driscoll, B. (2009) Lung alveolar integrity is compromised by telomere shortening in telomerase-null mice. *Am. J. Physiol. Lung Cell. Mol. Physiol.* **296,** L57–L70
26. Jackson, S. R., Lee, J., Reddy, R., Williams, G. N., Kikuchi, A., Freiberg, Y., Warburton, D., and Driscoll, B. (2011) Partial pneumonectomy of telomerase null mice carrying shortened telomeres initiates cell growth arrest resulting in a limited compensatory growth response. *Am. J. Physiol. Lung Cell. Mol. Physiol.* **300,** L898–L909
27. Alder, J. K., Guo, N., Kembou, F., Parry, E. M., Anderson, C. J., Gorgy, A. I., Walsh, M. F., Sussan, T., Biswal, S., Mitzner, W., Tuder, R. M., and Armanios, M. (2011) Telomere length is a determinant of emphysema susceptibility. *Am. J. Respir. Crit. Care Med.* **184,** 904–912
28. Liu, T., Chung, M. J., Ullenbruch, M., Yu, H., Jin, H., Hu, B., Choi, Y. Y., Ishikawa, F., and Phan, S. H. (2007) Telomerase activity is required for bleomycin-induced pulmonary fibrosis in mice. *J. Clin. Invest.* **117,** 3800–3809
29. Nozaki, Y., Liu, T., Hatano, K., Gharaee-Kermani, M., and Phan, S. H. (2000) Induction of telomerase activity in fibroblasts from bleomycin-injured lungs. *Am. J. Respir. Cell Mol. Biol.* **23,** 460–465
30. Liu, T., Ullenbruch, M., Young Choi, Y., Yu, H., Ding, L., Xaubet, A., Pereda, J., Feghali-Bostwick, C. A., Bitterman, P. B., Henke, C. A., Pardo, A., Selman, M., and Phan, S. H. (2013) Telomerase and telomere length in pulmonary fibrosis. *Am. J. Respir. Cell Mol. Biol.* **49,** 260–268
31. Erdmann, N., Liu, Y., and Harrington, L. (2004) Distinct dosage requirements for the maintenance of long and short telomeres in mTert heterozygous mice. *Proc. Natl. Acad. Sci. U.S.A.* **101,** 6080–6085
32. Reddy, R., Buckley, S., Doerken, M., Barsky, L., Weinberg, K., Anderson, K. D., Warburton, D., and Driscoll, B. (2004) Isolation of a putative progenitor subpopulation of alveolar epithelial type 2 cells. *Am. J. Physiol. Lung Cell. Mol. Physiol.* **286,** L658–L667
33. Lee, J., Reddy, R., Barsky, L., Weinberg, K., and Driscoll, B. (2006) Contribution of proliferation and DNA damage repair to alveolar epithelial type 2 cell recovery from hyperoxia. *Am. J. Physiol. Lung Cell. Mol. Physiol.* **290,** L685–L694
34. Kurz, D. J., Decary, S., Hong, Y., and Erusalimsky, J. D. (2000) Senescence-associated β-galactosidase reflects an increase in lysosomal mass during replicative ageing of human endothelial cells. *J. Cell Sci.* **113,** 3613–3622
35. Fujitani, Y., Kanaoka, Y., Aritake, K., Uodome, N., Okazaki-Hatake, K., and Urade, Y. (2002) Pronounced eosinophilic lung inflammation and Th2 cytokine release in human lipocalin-type prostaglandin D synthase transgenic mice. *J. Immunol.* **168,** 443–449
36. Zhou, B., Comeau, M. R., De Smedt, T., Liggitt, H. D., Dahl, M. E., Lewis, D. B., Gyarmati, D., Aye, T., Campbell, D. J., and Ziegler, S. F. (2005) Thymic stromal lymphopoietin as a key initiator of allergic airway inflammation in mice. *Nat. Immunol.* **6,** 1047–1053
37. Driscoll, B., Buckley, S., Bui, K. C., Anderson, K. D., and Warburton, D. (2000) Telomerase in alveolar epithelial development and repair. *Am. J. Physiol. Lung Cell. Mol. Physiol.* **279,** L1191–L1198
38. Amsellem, V., Gary-Bobo, G., Marcos, E., Maitre, B., Chaar, V., Validire, P., Stern, J. B., Noureddine, H., Sapin, E., Rideau, D., Hue, S., Le Corvoisier, P., Le Gouvello, S., Dubois-Randé, J. L., Boczkowski, J., and Adnot, S. (2011) Telomere dysfunction causes sustained inflammation in chronic obstructive pulmonary disease. *Am. J. Respir. Crit. Care Med.* **184,** 1358–1366
39. Schneider, D. J., Wu, M., Le, T. T., Cho, S. H., Brenner, M. B., Blackburn, M. R., and Agarwal, S. K. (2012) Cadherin-11 contributes to pulmonary fibrosis: potential role in TGF-β production and epithelial to mesenchymal transition. *FASEB J.* **26,** 503–512
40. Song, X., Liu, W., Xie, S., Wang, M., Cao, G., Mao, C., and Lv, C. (2013) All-*trans*-retinoic acid ameliorates bleomycin-induced lung fibrosis by downregulating the TGF-β1/Smad3 signaling pathway in rats. *Lab. Invest.* **93,** 1219–1231
41. Zhou, H., Liao, J., Aloor, J., Nie, H., Wilson, B. C., Fessler, M. B., Gao, H. M., and Hong, J. S. (2013) CD11b/CD18 (Mac-1) is a novel surface receptor for extracellular double-stranded RNA to mediate cellular inflammatory responses. *J. Immunol.* **190,** 115–125
42. Huaux, F., Lo Re, S., Giordano, G., Uwambayinema, F., Devosse, R., Yakoub, Y., Panin, N., Palmai-Pallag, M., Rabolli, V., Delos, M., Marbaix, E., Dauguet, N., Couillin, I., Ryffel, B., Renauld, J. C., and Lison, D. (2015) IL-1α induces CD11b(low) alveolar macrophage proliferation and maturation during granuloma formation. *J. Pathol.* **235,** 698–709
43. Kim, J. K., Lim, Y., Kim, K. A., Seo, M. S., Kim, J. D., Lee, K. H., and Park, C. Y. (2000) Activation of telomerase by silica in rat lung. *Toxicol. Lett.* **111,** 263–270
44. Fridlender, Z. G., Cohen, P. Y., Golan, O., Arish, N., Wallach-Dayan, S., and Breuer, R. (2007) Telomerase activity in bleomycin-induced epithelial cell apoptosis and lung fibrosis. *Eur. Respir. J.* **30,** 205–213
45. Degryse, A. L., Xu, X. C., Newman, J. L., Mitchell, D. B., Tanjore, H., Polosukhin, V. V., Jones, B. R., McMahon, F. B., Gleaves, L. A., Phillips, J. A., 3rd, Cogan, J. D., Blackwell, T. S., and Lawson, W. E. (2012) Telomerase deficiency does not alter bleomycin-induced fibrosis in mice. *Exp. Lung Res.* **38,** 124–134
46. Nunes, H., Monnet, I., Kannengiesser, C., Uzunhan, Y., Valeyre, D., Kambouchner, M., and Naccache, J. M. (2014) Is telomeropathy the explanation for combined pulmonary fibrosis and emphysema syndrome?: report of a family with TERT mutation. *Am. J. Respir. Crit. Care Med.* **189,** 753–754
47. Stanley, S. E., Chen, J. J., Podlevsky, J. D., Alder, J. K., Hansel, N. N., Mathias, R. A., Qi, X., Rafaels, N. M., Wise, R. A., Silverman, E. K., Barnes, K. C., and Armanios, M. (2015) Telomerase mutations in smokers with severe emphysema. *J. Clin. Invest.* **125,** 563–570
48. Barkauskas, C. E., Cronce, M. J., Rackley, C. R., Bowie, E. J., Keene, D. R., Stripp, B. R., Randell, S. H., Noble, P. W., and Hogan, B. L. (2013) Type 2 alveolar cells are stem cells in adult lung. *J. Clin. Invest.* **123,** 3025–3036
49. Desai, T. J., Brownfield, D. G., and Krasnow, M. A. (2014) Alveolar progenitor and stem cells in lung development, renewal and cancer. *Nature* **507,** 190–194
50. Waisberg, D. R., Barbas-Filho, J. V., Parra, E. R., Fernezlian, S., de Carvalho, C. R., Kairalla, R. A., and Capelozzi, V. L. (2010) Abnormal expression of

telomerase/apoptosis limits type II alveolar epithelial cell replication in the early remodeling of usual interstitial pneumonia/idiopathic pulmonary fibrosis. *Hum. Pathol.* **41,** 385–391
51. Alder, J. K., Barkauskas, C. E., Limjunyawong, N., Stanley, S. E., Kembou, F., Tuder, R. M., Hogan, B. L., Mitzner, W., and Armanios, M. (2015) Telomere dysfunction causes alveolar stem cell failure. *Proc. Natl. Acad. Sci. U.S.A.* **112,** 5099–5104
52. Watanabe-Takano, H., Takano, K., Hatano, M., Tokuhisa, T., and Endo, T. (2015) DA-Raf-mediated suppression of the Ras-ERK pathway is essential for TGF-β1-induced epithelial-mesenchymal transition in alveolar epithelial type 2 cells. *PLoS One* **10,** e0127888
53. Maida, Y., Kyo, S., Kanaya, T., Wang, Z., Yatabe, N., Tanaka, M., Nakamura, M., Ohmichi, M., Gotoh, N., Murakami, S., and Inoue, M. (2002) Direct activation of telomerase by EGF through Ets-mediated transactivation of TERT via MAP kinase signaling pathway. *Oncogene* **21,** 4071–4079
54. Xu, D., Dwyer, J., Li, H., Duan, W., and Liu, J. P. (2008) Ets2 maintains hTERT gene expression and breast cancer cell proliferation by interacting with c-Myc. *J. Biol. Chem.* **283,** 23567–23580
55. Cassar,L.,Li,H.,Jiang,F.X.,andLiu,J.P.(2010)TGF-βinducestelomerase-dependent pancreatic tumor cell cycle arrest. *Mol. Cell. Endocrinol.* **320,** 97–105
56. Li, H., Xu, D., Li, J., Berndt, M. C., and Liu, J. P. (2006) Transforming growth factor β suppresses human telomerase reverse transcriptase (hTERT) by Smad3 interactions with c-Myc and the hTERT gene. *J. Biol. Chem.* **281,** 25588–25600
57. Yang, H., Kyo, S., Takatura, M., and Sun, L. (2001) Autocrine transforming growth factor β suppresses telomerase activity and transcription of human telomerase reverse transcriptase in human cancer cells. *Cell Growth Differ.* **12,** 119–127
58. Zhang, F., Nielsen, L. D., Lucas, J. J., and Mason, R. J. (2004) Transforming growth factor-β antagonizes alveolar type II cell proliferation induced by keratinocyte growth factor. *Am. J. Respir. Cell Mol. Biol.* **31,** 679–686
59. Kasai, H., Allen, J. T., Mason, R. M., Kamimura, T., and Zhang, Z. (2005) TGF-β1 induces human alveolar epithelial to mesenchymal cell transition (EMT). *Respir. Res.* **6,** 56
60. Bhaskaran, M., Kolliputi, N., Wang, Y., Gou, D., Chintagari, N. R., and Liu, L. (2007) Trans-differentiation of alveolar epithelial type II cells to type I cells involves autocrine signaling by transforming growth factor β1 through the Smad pathway. *J. Biol. Chem.* **282,** 3968–3976
61. Alipio, Z. A., Jones, N., Liao, W., Yang, J., Kulkarni, S., Sree Kumar, K., Hauer-Jensen, M., Ward, D. C., Ma, Y., and Fink, L. M. (2011) Epithelial to mesenchymal transition (EMT) induced by bleomycin or TFG(b1)/EGF in murine induced pluripotent stem cell-derived alveolar type II-like cells. *Differentiation* **82,** 89–98
62. Zhao, L., Yee, M., and O'Reilly, M. A. (2013) Transdifferentiation of alveolar epithelial type II to type I cells is controlled by opposing TGF-β and BMP signaling. *Am. J. Physiol. Lung Cell. Mol. Physiol.* **305,** L409–L418
63. Warburton, D., Shi, W., and Xu, B. (2013) TGF-β-Smad3 signaling in emphysema and pulmonary fibrosis: an epigenetic aberration of normal development? *Am. J. Physiol. Lung Cell. Mol. Physiol.* **304,** L83–L85
64. Li, M., Krishnaveni, M. S., Li, C., Zhou, B., Xing, Y., Banfalvi, A., Li, A., Lombardi, V., Akbari, O., Borok, Z., and Minoo, P. (2011) Epithelium-specific deletion of TGF-β receptor type II protects mice from bleomycin-induced pulmonary fibrosis. *J. Clin. Invest.* **121,** 277–287
65. Willis, B. C., Liebler, J. M., Luby-Phelps, K., Nicholson, A. G., Crandall, E. D., du Bois, R. M., and Borok, Z. (2005) Induction of epithelial-mesenchymal transition in alveolar epithelial cells by transforming growth factor-β1: potential role in idiopathic pulmonary fibrosis. *Am. J. Pathol.* **166,** 1321–1332
66. Zhou, B., Liu, Y., Kahn, M., Ann, D. K., Han, A., Wang, H., Nguyen, C., Flodby, P., Zhong, Q., Krishnaveni, M. S., Liebler, J. M., Minoo, P., Crandall, E. D., and Borok, Z. (2012) Interactions between β-catenin and transforming growth factor-β signaling pathways mediate epithelial-mesenchymal transition and are dependent on the transcriptional co-activator cAMP-response element-binding protein (CREB)-binding protein (CBP). *J. Biol. Chem.* **287,** 7026–7038
67. Rahaman, S. O., Grove, L. M., Paruchuri, S., Southern, B. D., Abraham, S., Niese, K. A., Scheraga, R. G., Ghosh, S., Thodeti, C. K., Zhang, D. X., Moran, M. M., Schilling, W. P., Tschumperlin, D. J., and Olman, M. A. (2014) TRPV4 mediates myofibroblast differentiation and pulmonary fibrosis in mice. *J. Clin. Invest.* **124,** 5225–5238
68. Chilosi, M., Poletti, V., and Rossi, A. (2012) The pathogenesis of COPD and IPF: distinct horns of the same devil? *Respir. Res.* **13,** 3
69. Kropski, J. A., Lawson, W. E., and Blackwell, T. S. (2012) Right place, right time: the evolving role of herpesvirus infection as a "second hit" in idiopathic pulmonary fibrosis. *Am. J. Physiol. Lung Cell. Mol. Physiol.* **302,** L441–L444
70. Kojima, H., Kunimoto, H., Inoue, T., and Nakajima, K. (2012) The STAT3-IGFBP5 axis is critical for IL-6/gp130-induced premature senescence in human fibroblasts. *Cell Cycle* **11,** 730–739
71. Savale, L., Chaouat, A., Bastuji-Garin, S., Marcos, E., Boyer, L., Maitre, B., Sarni, M., Housset, B., Weitzenblum, E., Matrat, M., Le Corvoisier, P., Rideau, D., Boczkowski, J., Dubois-Randé, J. L., Chouaid, C., and Adnot, S. (2009) Shortened telomeres in circulating leukocytes of patients with chronic obstructive pulmonary disease. *Am. J. Respir. Crit. Care Med.* **179,** 566–571
72. Rodier, F., Coppé, J. P., Patil, C. K., Hoeijmakers, W. A., Muñoz, D. P., Raza, S. R., Freund, A., Campeau, E., Davalos, A. R., and Campisi, J. (2009) Persistent DNA damage signalling triggers senescence-associated inflammatory cytokine secretion. *Nat. Cell Biol.* **11,** 973–979
73. Damjanovic, A. K., Yang, Y., Glaser, R., Kiecolt-Glaser, J. K., Nguyen, H., Laskowski, B., Zou, Y., Beversdorf, D. Q., and Weng, N. P. (2007) Accelerated telomere erosion is associated with a declining immune function of caregivers of Alzheimer's disease patients. *J. Immunol.* **179,** 4249–4254
74. Iannello, A., and Raulet, D. H. (2014) Immunosurveillance of senescent cancer cells by natural killer cells. *Oncoimmunology* **3,** e27616
75. Jurk, D., Wilson, C., Passos, J. F., Oakley, F., Correia-Melo, C., Greaves, L., Saretzki, G., Fox, C., Lawless, C., Anderson, R., Hewitt, G., Pender, S. L., Fullard, N., Nelson, G., Mann, J., van de Sluis, B., Mann, D. A., and von Zglinicki, T. (2014) Chronic inflammation induces telomere dysfunction and accelerates ageing in mice. *Nat. Commun.* **2,** 4172
76. Robin, J. D., Ludlow, A. T., Batten, K., Magdinier, F., Stadler, G., Wagner, K. R., Shay, J. W., and Wright, W. E. (2014) Telomere position effect: regulation of gene expression with progressive telomere shortening over long distances. *Genes Dev.* **28,** 2464–2476
77. Arnoult, N., Van Beneden, A., and Decottignies, A. (2012) Telomere length regulates TERRA levels through increased trimethylation of telomeric H3K9 and HP1α. *Nat. Struct. Mol. Biol.* **19,** 948–956
78. Kaczorowski, D. J., Scott, M. J., Pibris, J. P., Afrazi, A., Nakao, A., Edmonds, R. D., Kim, S., Kwak, J. H., Liu, Y., Fan, J., and Billiar, T. R. (2012) Mammalian DNA is an endogenous danger signal that stimulates local synthesis and release of complement factor B. *Mol. Med.* **18,** 851–860
79. Zhang, Q., Raoof, M., Chen, Y., Sumi, Y., Sursal, T., Junger, W., Brohi, K., Itagaki, K., and Hauser, C. J. (2010) Circulating mitochondrial DAMPs cause inflammatory responses to injury. *Nature* **464,** 104–107